

2017
光物性物理学
Optical Properties and Spectroscopy of Materials

松田巖

Lecture Note 4

X-ray Absorption spectroscopy
and
X-ray emission spectroscopy

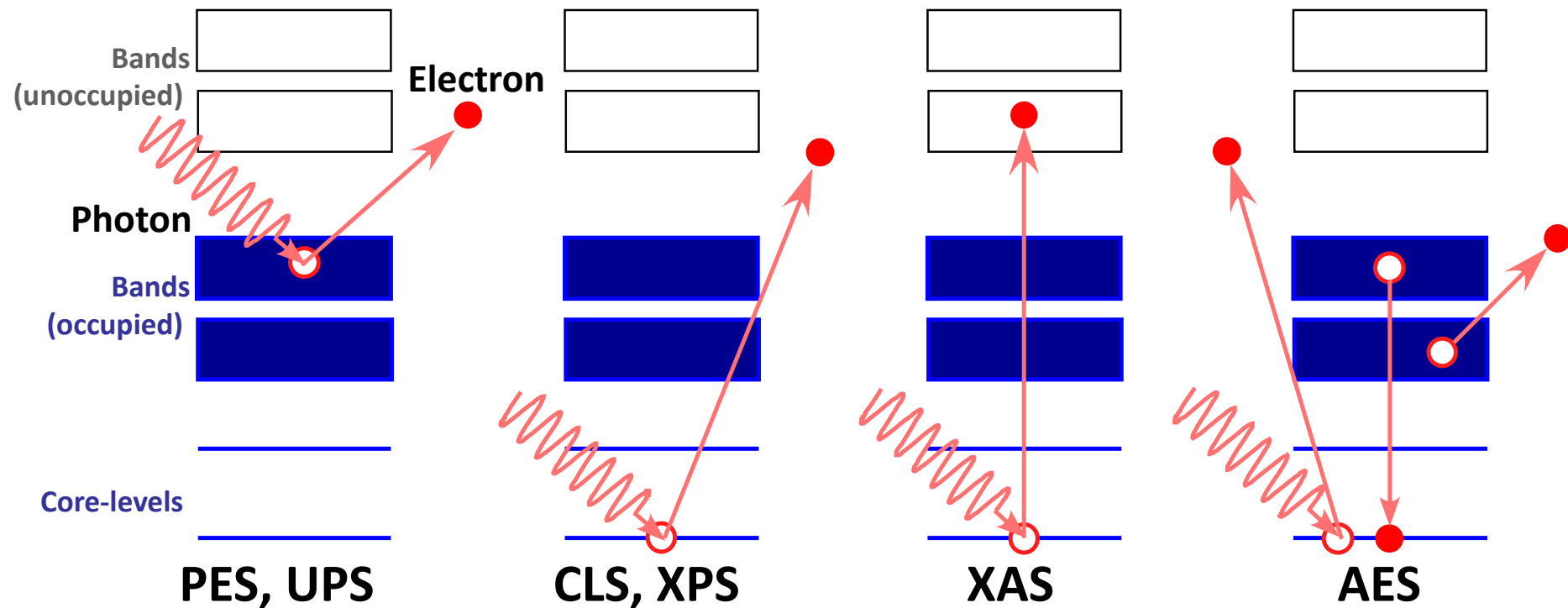
Photon-in / Particle-out

Photoemission Spectroscopy (PES), Ultraviolet Photoelectron Spectroscopy (UPS)

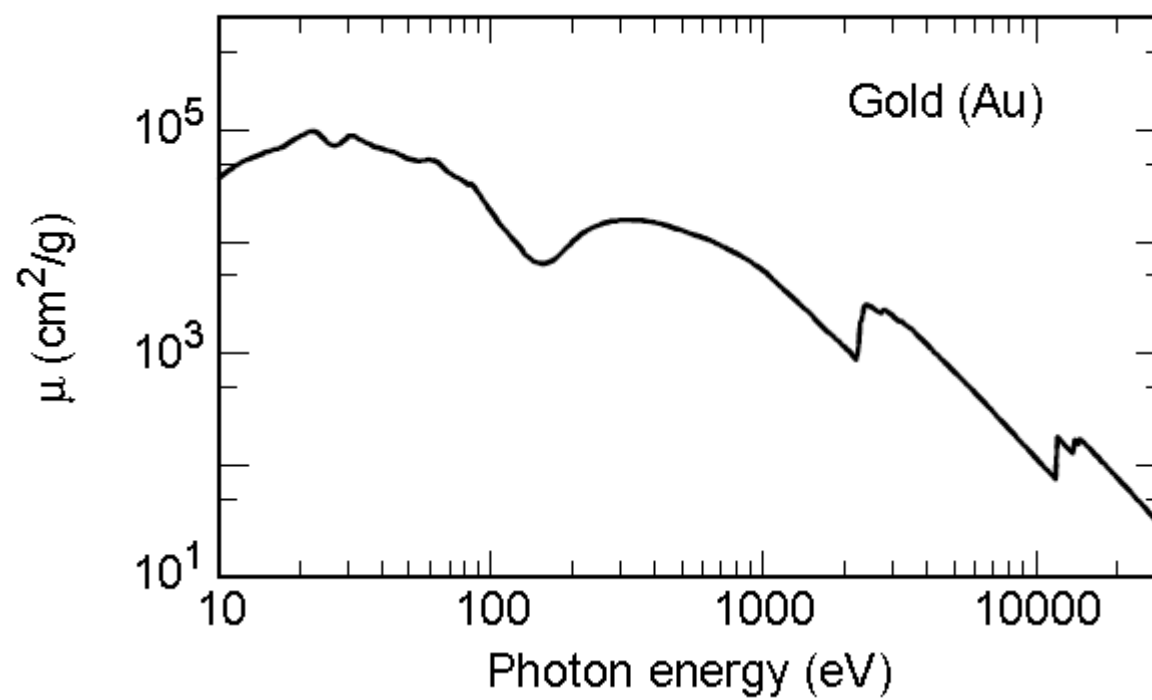
Core-level Spectroscopy (CLS), X-ray Photoelectron Spectroscopy (XPS)

X-ray Absorption Spectroscopy (XAS)

Auger Electron Spectroscopy (AES)

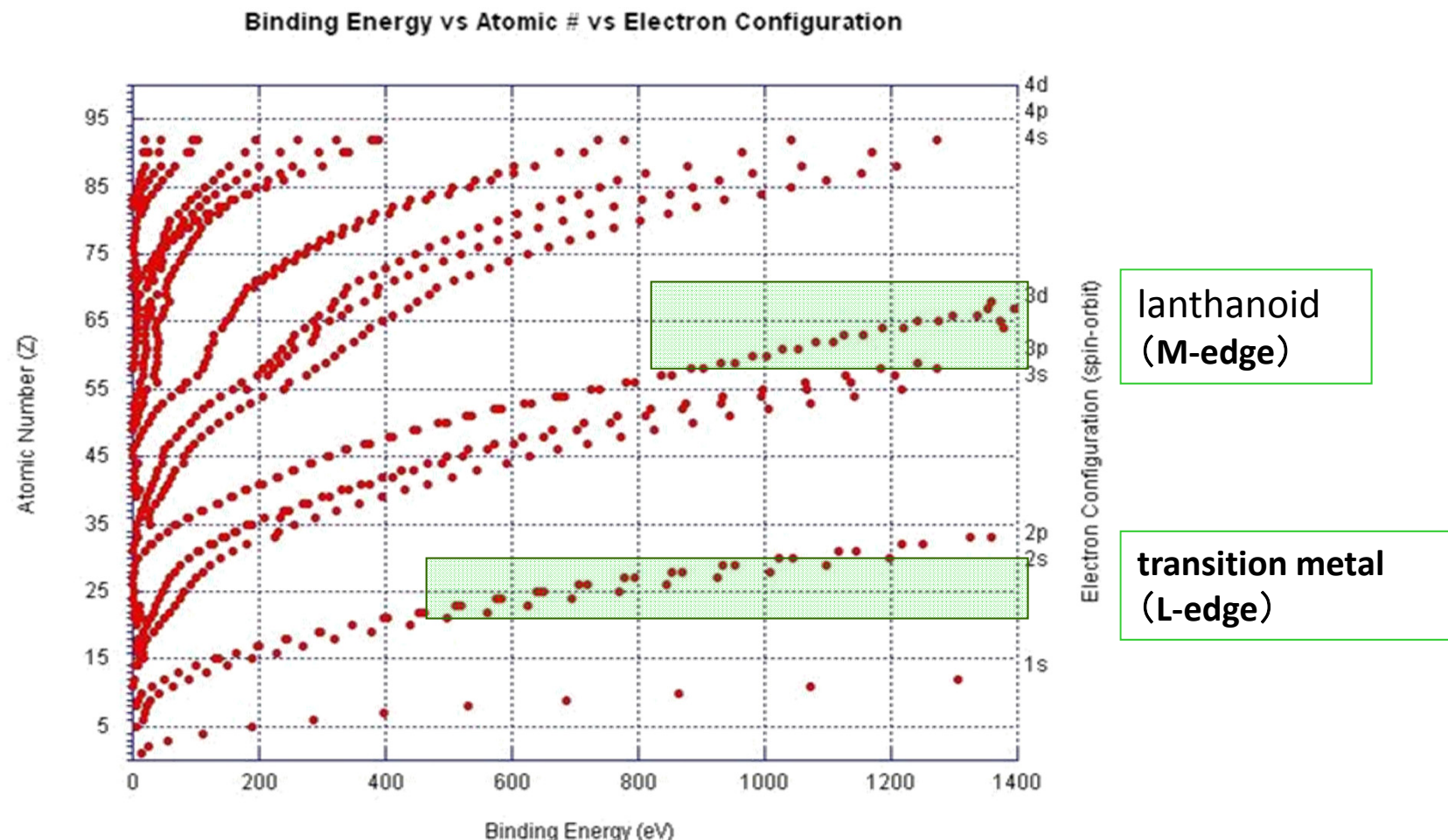


質量吸收係數: μ (cm^2/g)



Spectroscopy with VUV~SX

- Absorption edge, resonance effect



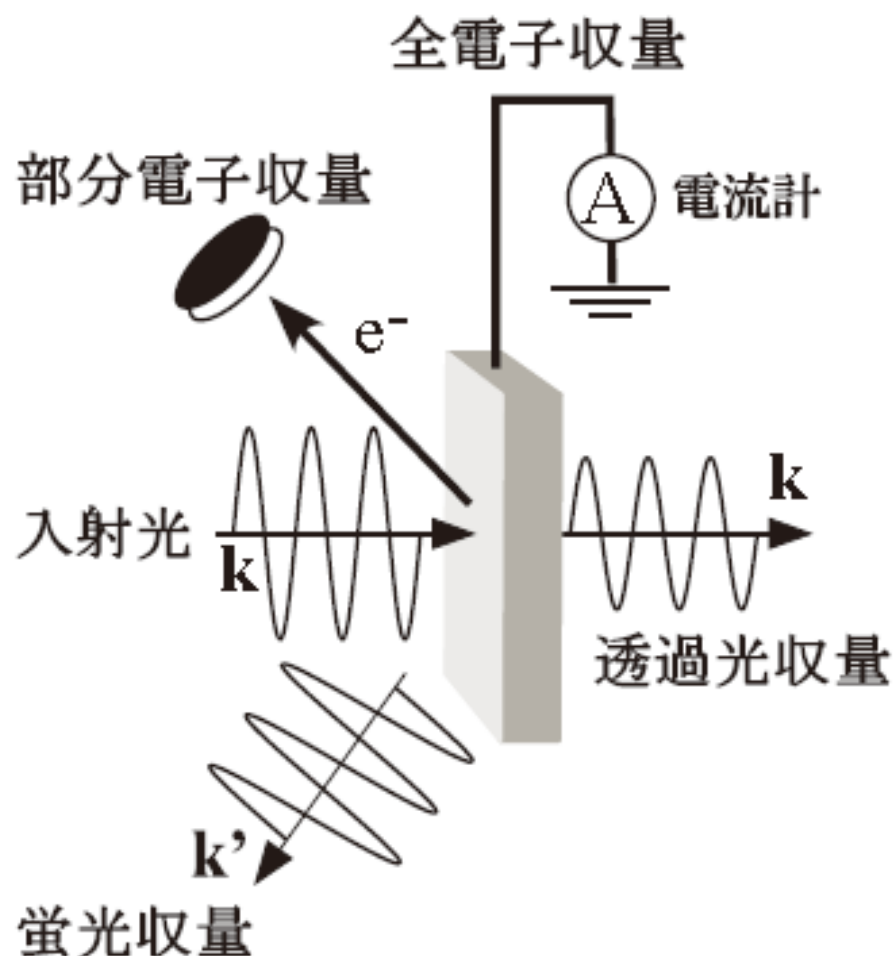


FIG. 19: X 線吸収分光実験の様子。

Transmission yield (透過光収量)

$$I_t = I_0 e^{-\mu t}$$

- Direct measurement
- Sample thickness limit ($\leq 100\text{nm}$)

Electron yield (電子収量)

$$I_e = I_0 \mu L_e$$

- Indirect measurement
- Rather surface sensitive (probing depth $\sim 5\text{nm}$)

Fluorescence yield (蛍光収量)

$$I_f = I_0 \mu L_f$$

- Indirect measurement
- Rather bulk sensitive
- Self-absorption problem

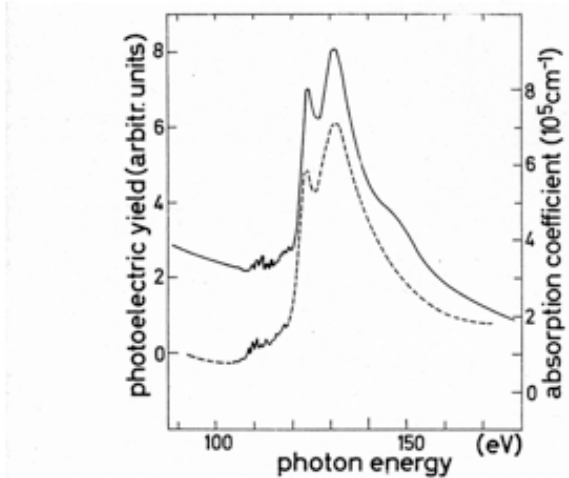


FIG. 1. Comparison of photoelectric yield (solid curve) and absorption (dashed curve) spectra for Pr.

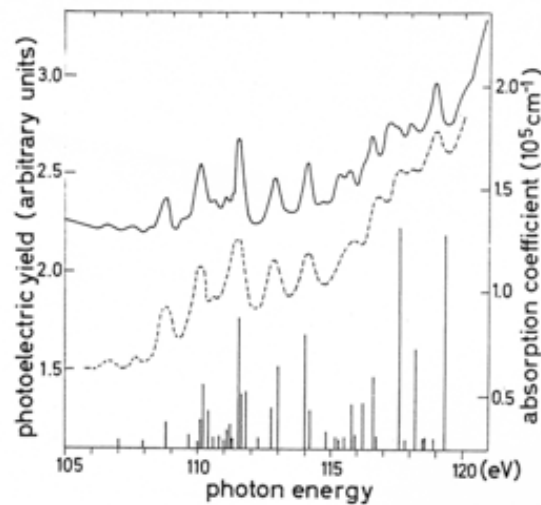
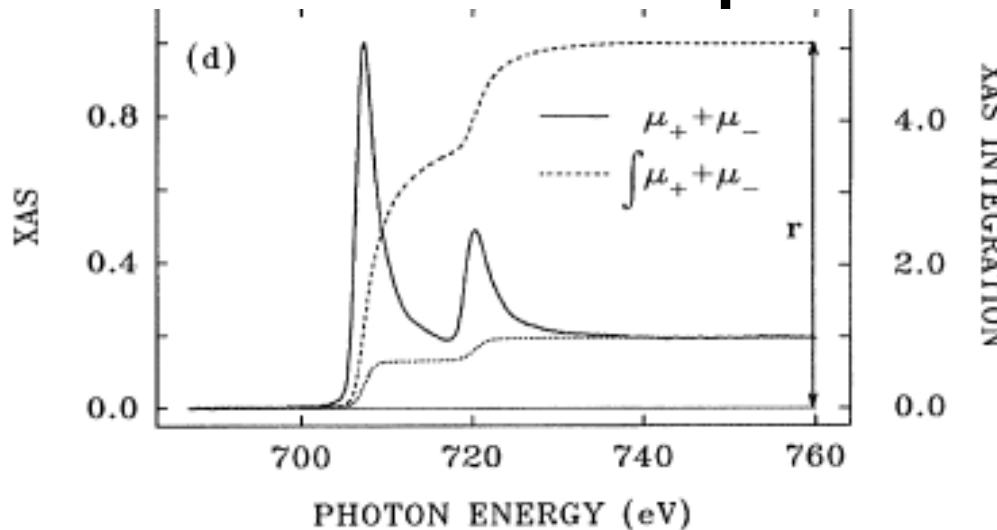


FIG. 2. Energy region of fine structure, yield (solid curve) and absorption (dashed curve) for Pr. The vertical lines are the result of an atomic calculation (Ref. 19); the length of the lines represents the oscillator strength.

透過法と電子収量法で測定したプラセオジウムの軟X線吸収スペクトル。
[W. Gudat and C. Kunz, *Phys. Rev. Lett.*, 29, 169-172 (1972)]

Example Fe and FeO



Fe:

C.T. Chen *et al.*, Phys. Rev. Lett. **75**, 152 (1995).

Fe₂O₃:

P. Kuiper *et al.*, Phys. Rev. Lett. **70**, 1549 (1993).

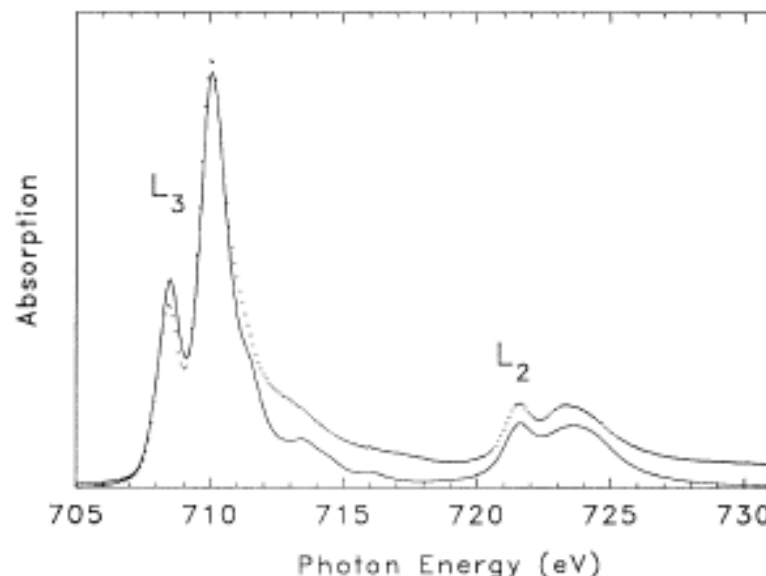
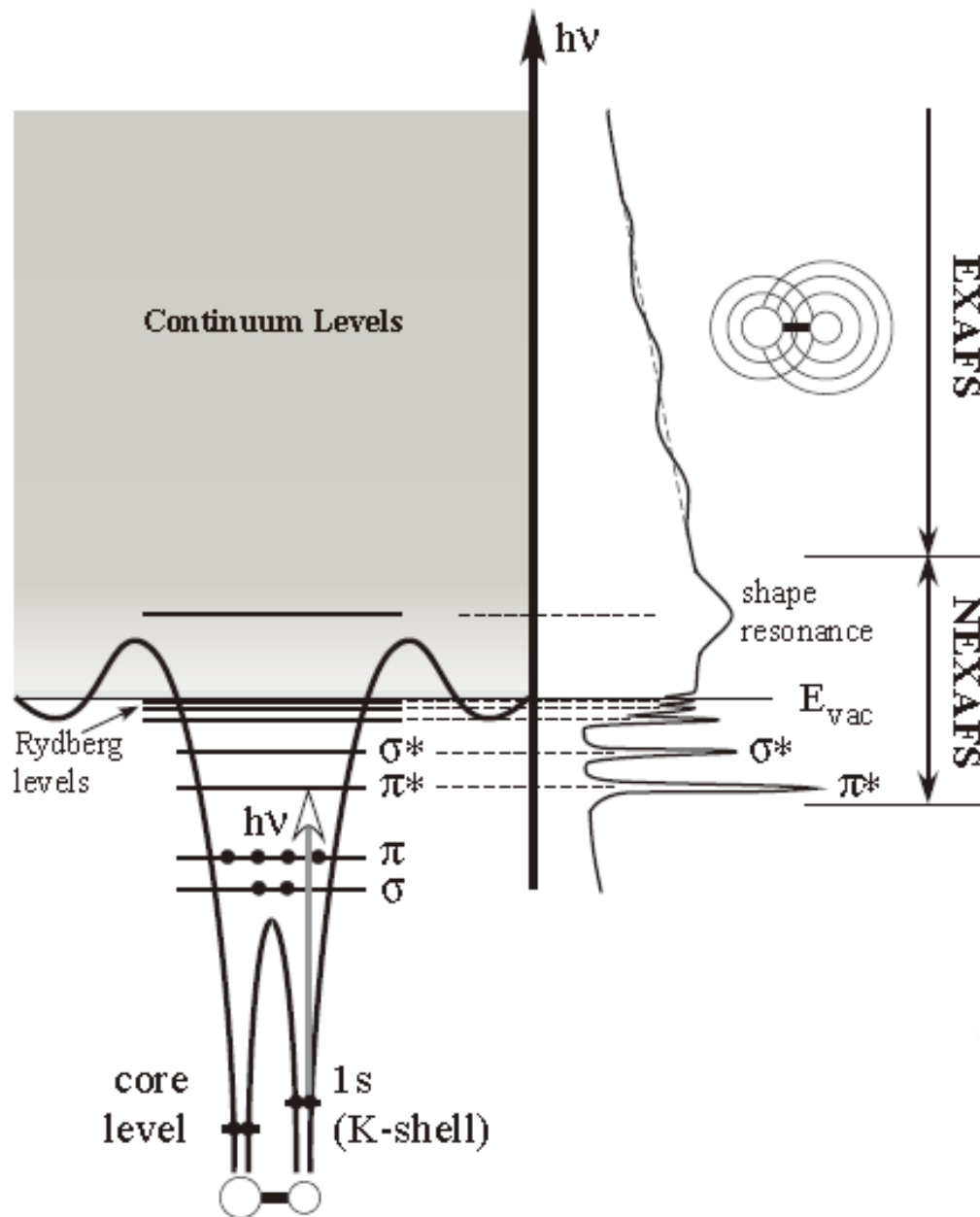


FIG. 1. Comparison of the Fe 2p absorption spectrum of Fe₂O₃ powder (points) with a calculation for Fe³⁺ (3d⁵) in octahedral symmetry (line).



Extended X-ray Absorption Fine Structure

Near-Edge X-ray Absorption Fine Structure

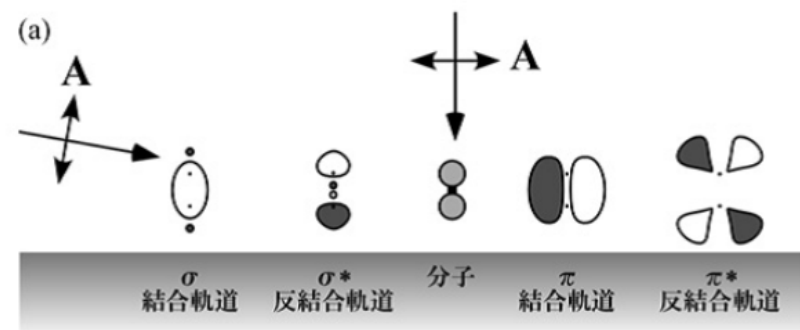


図 0.27 吸収端近傍における吸収スペクトルの様子。

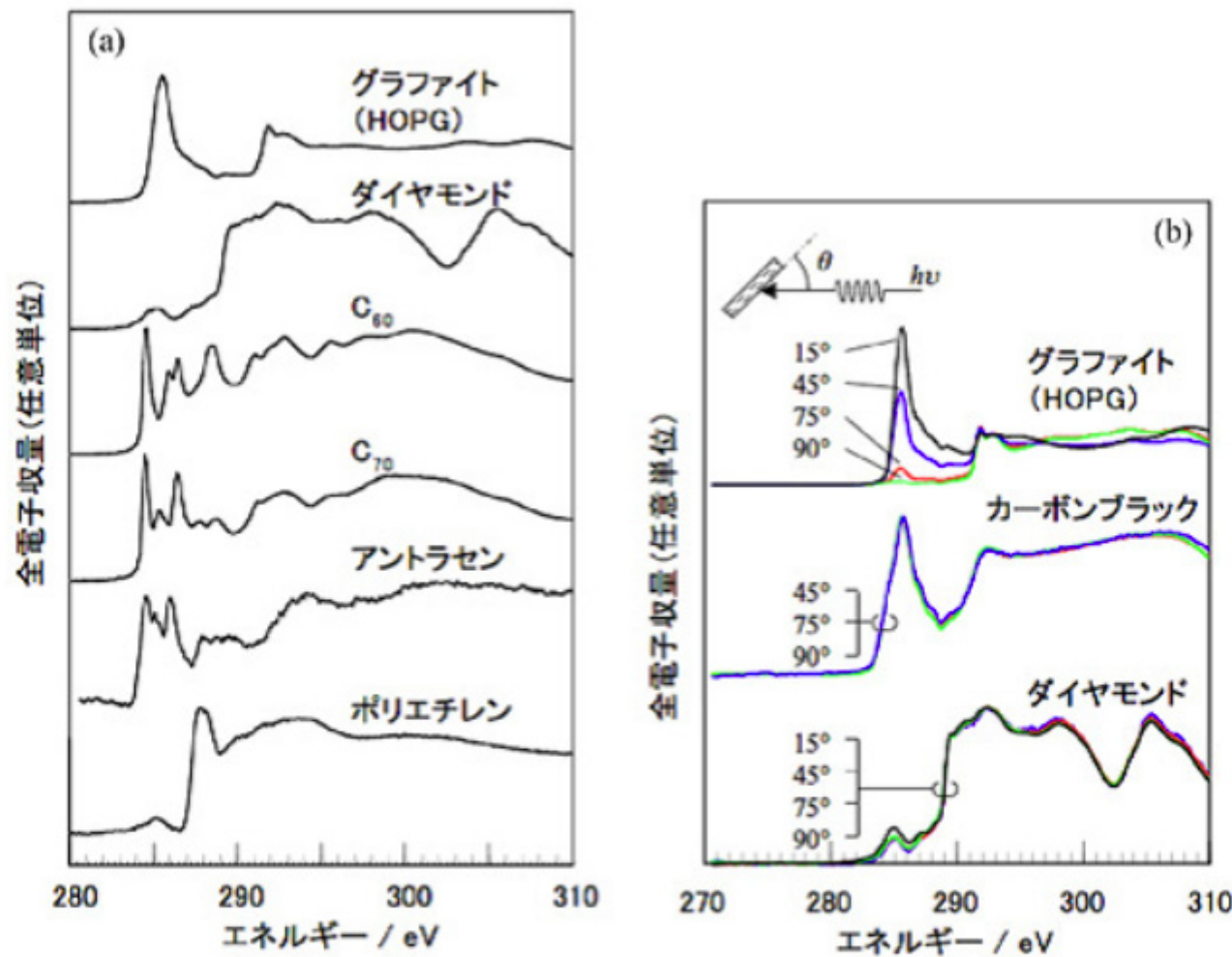
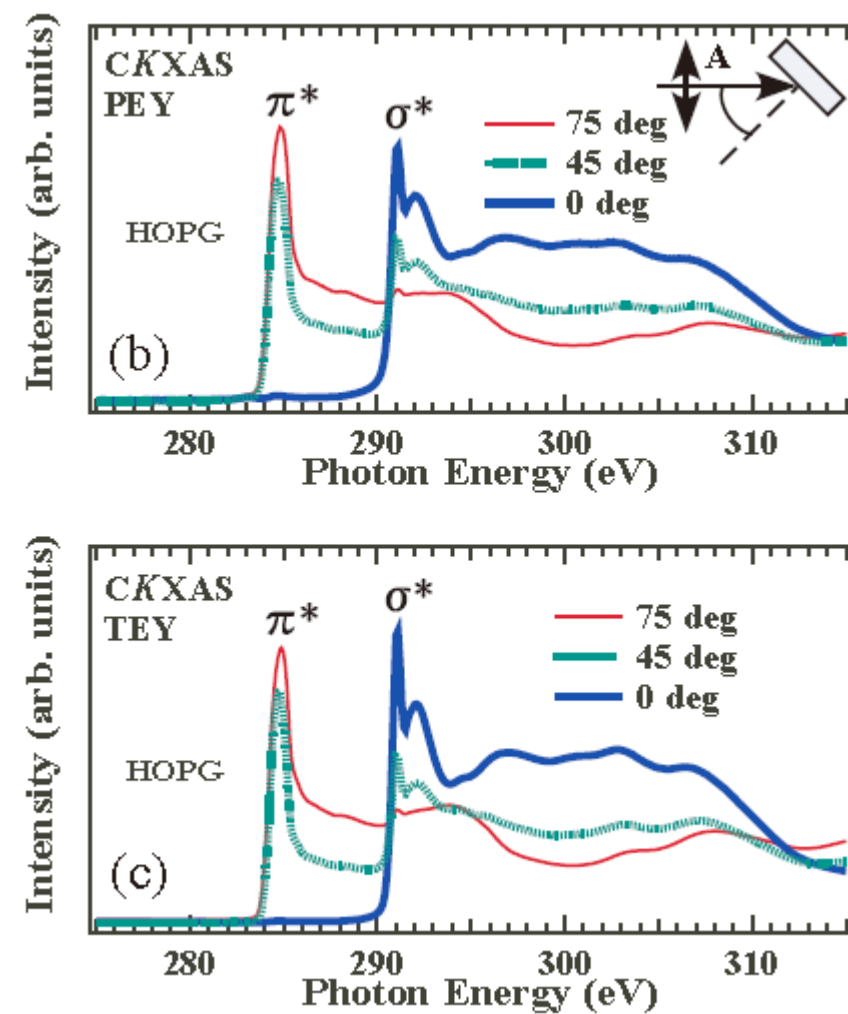
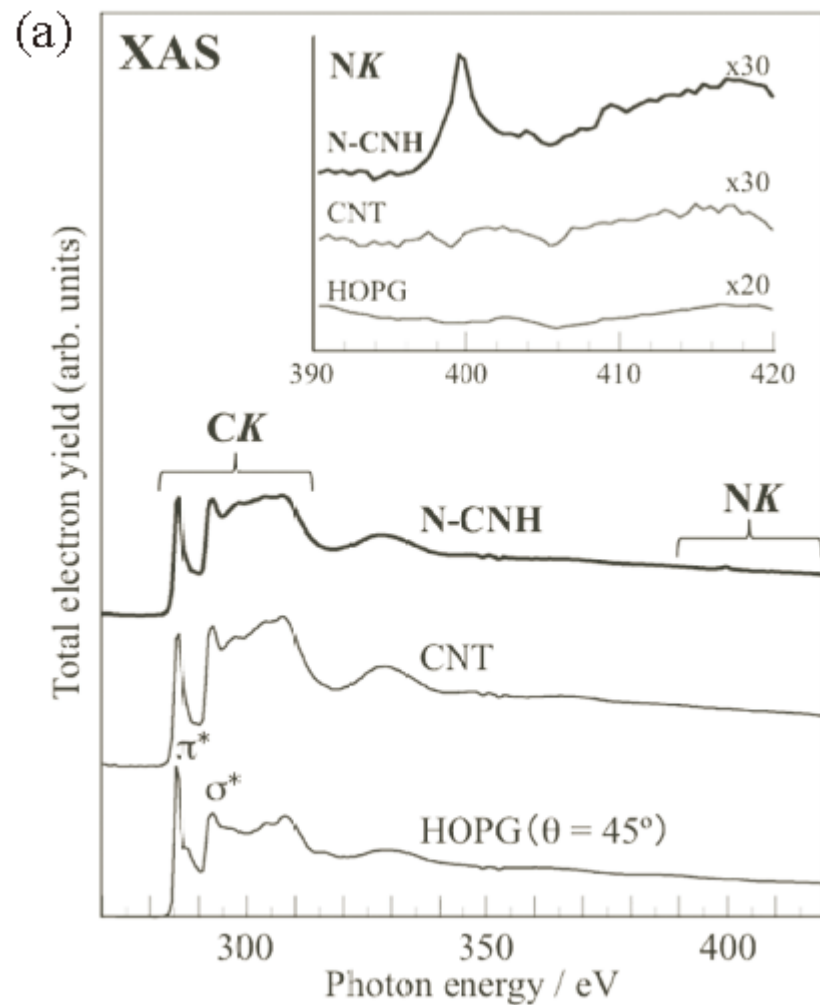
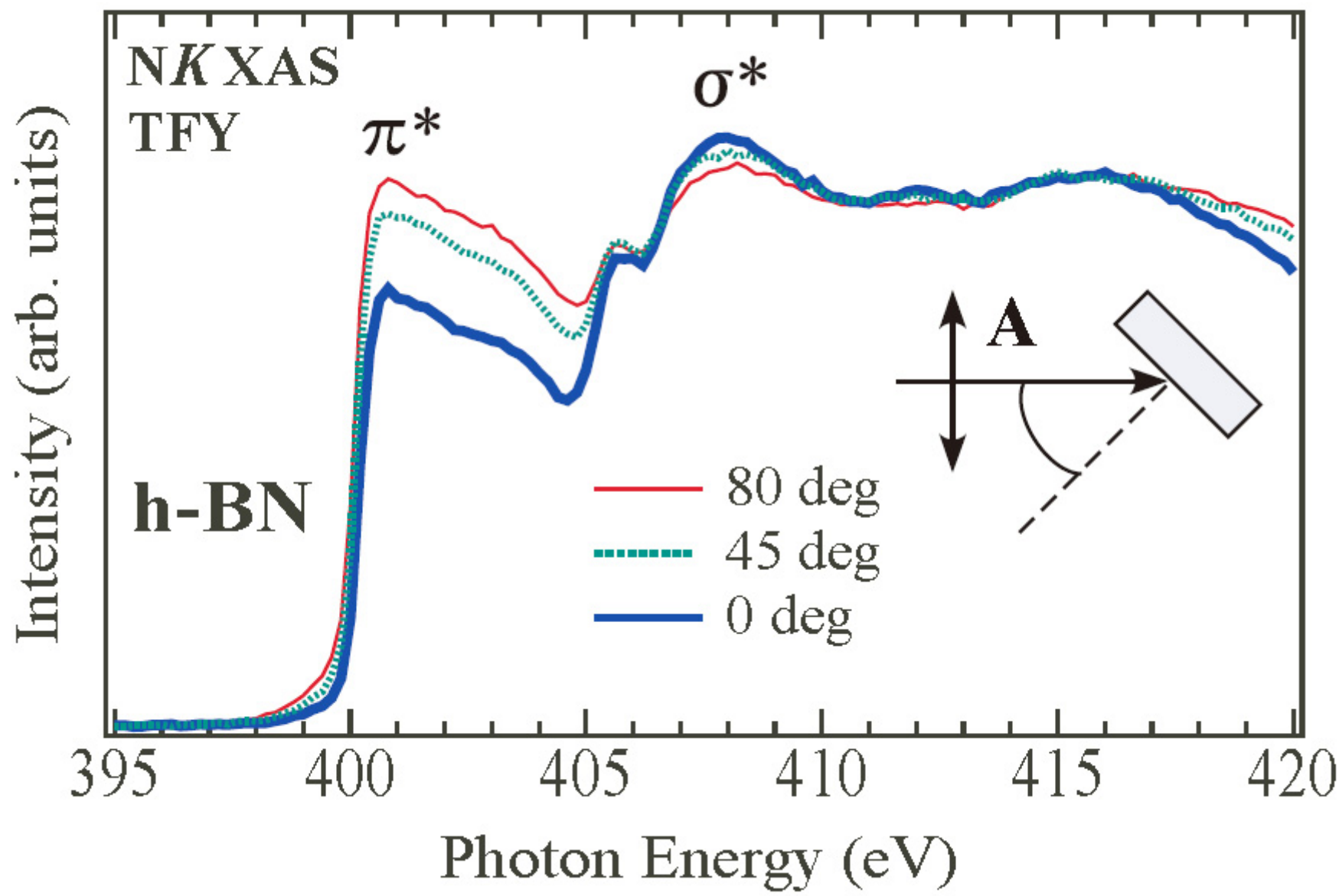
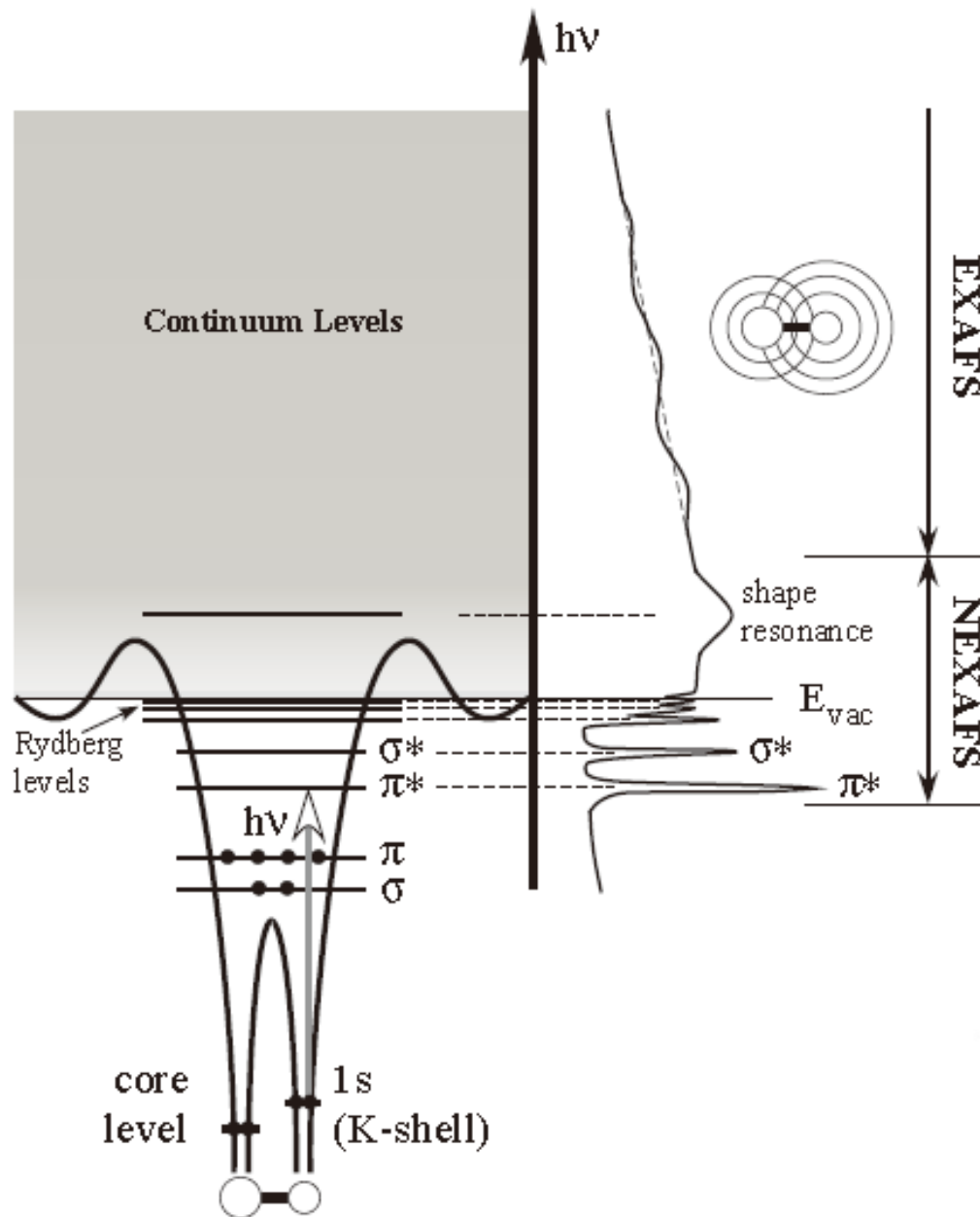


FIG. 20: (a) C K 吸收端における典型的炭素化合物の全電子吸収量軟X線吸収スペクトル。(b) 入射角 θ を変化させて測定したグラファイト、カーボンブラック、ダイヤモンドの軟X線吸収スペクトル。
(兵庫県立大：村松康司教授より提供)







Extended X-ray Absorption Fine Structure

Near-Edge X-ray Absorption Fine Structure

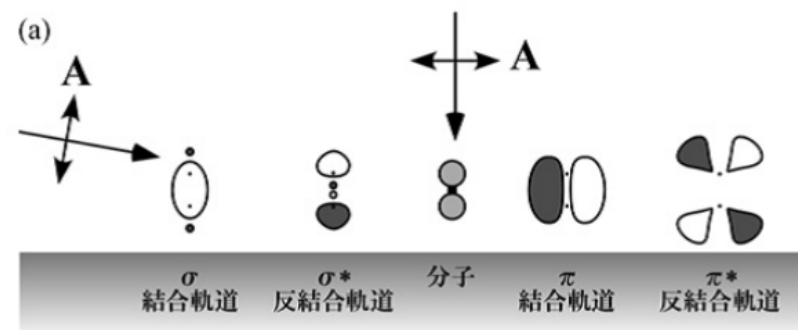


図 0.27 吸収端近傍における吸収スペクトルの様子。

EXAFS解析の流れ (Flow of EXAFS analysis)

1. 測定 (Measurement)
2. 実験データより $\chi(E)$ を取り出す (Extracting $\chi(E)$)
3. 波数スペクトルに変換して、重みを付けた $k^n \chi(k)$ をフーリエ変換し、大まかに原子構造を捉える。
(Conversion to wave vector spectra and Fourier transform $k^n \chi(k)$ to determine atomic structure roughly)
4. $\chi(k)$ を原子構造モデルを元にフィッティングする。
(Determine the accurate atomic structure by fitting $\chi(k)$)

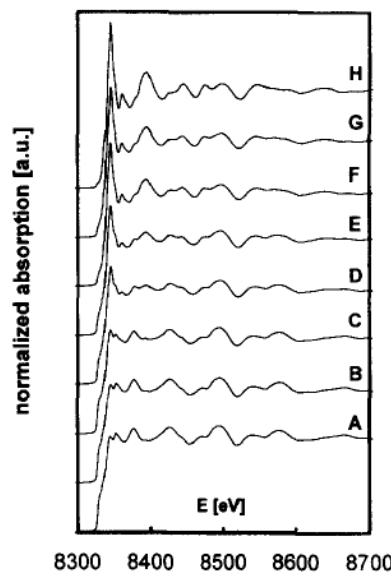


Fig. 1. Representative pre-edge background subtracted XAFS data (truncated at 8700 eV for clarity). A, B, D, F: CEY data. C, E, G, H: TEY data. NiO overlayer thicknesses: native oxide $\approx 25 \text{ \AA}$ (A), 50 \AA (B/C), 235 \AA (D/E), 1275 \AA (F/G), 3000 \AA (H).

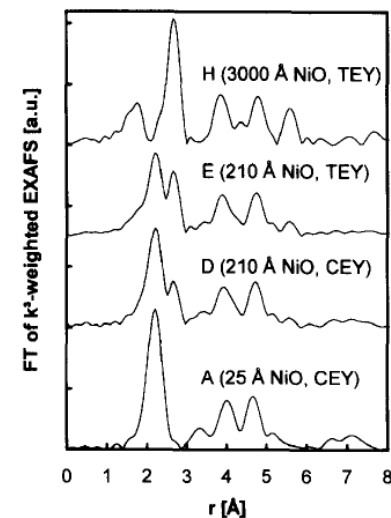


Fig. 2. Fourier transforms of k^3 -weighted EXAFS from spectra A, D, E and H of Fig. 1.

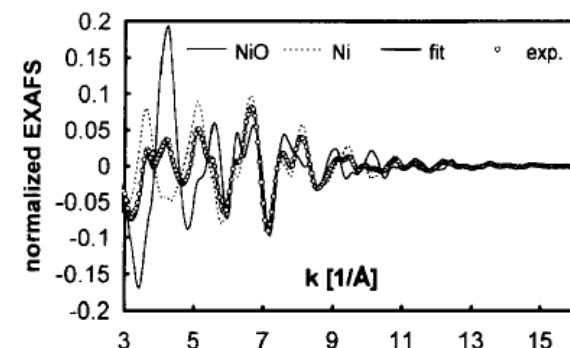
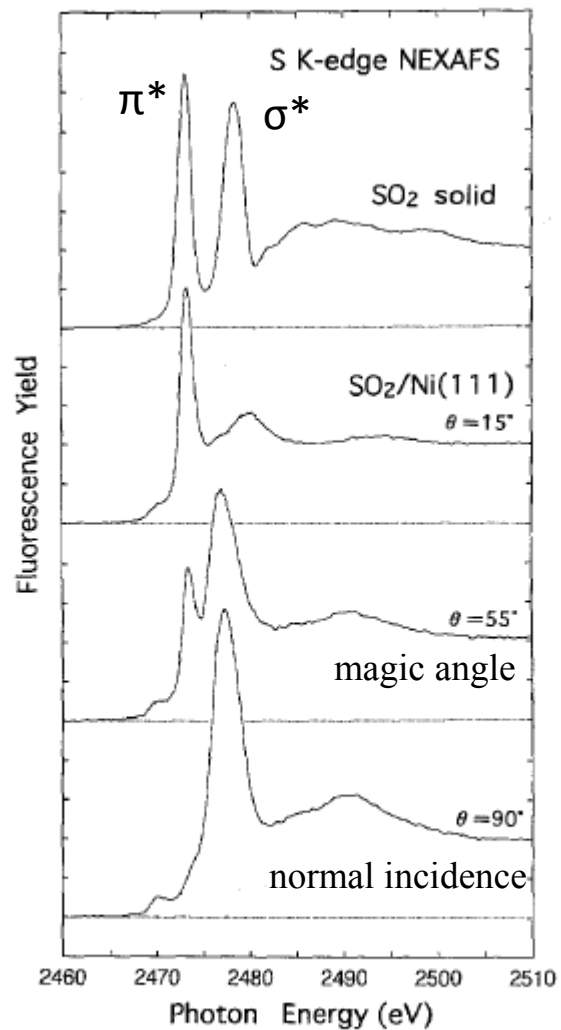


Fig. 3. Unweighted EXAFS from spectra A (dotted line), H (thin full line) and D (white circles) in Fig. 1. Thick full line: spectrum generated by linear combination of the EXAFS of A (35%) and H (65%).



- Suppression of the π^* peak
=> Partial occupation of the π^* orbital
=> Charge transfer from the Ni d-band
=> The strong mixing of $\text{SO}_2 \pi^*$ - Ni d-band

A flat-lying orientation
of the molecular plane on a surface

Fig. 1. S K-edge NEXAFS spectra of submonolayer $\text{SO}_2/\text{Ni}(111)$ taken at X-ray incidence angles of $\theta = 90^\circ$, 55° and 15° at a temperature of 92 K, together with that of solid SO_2 .

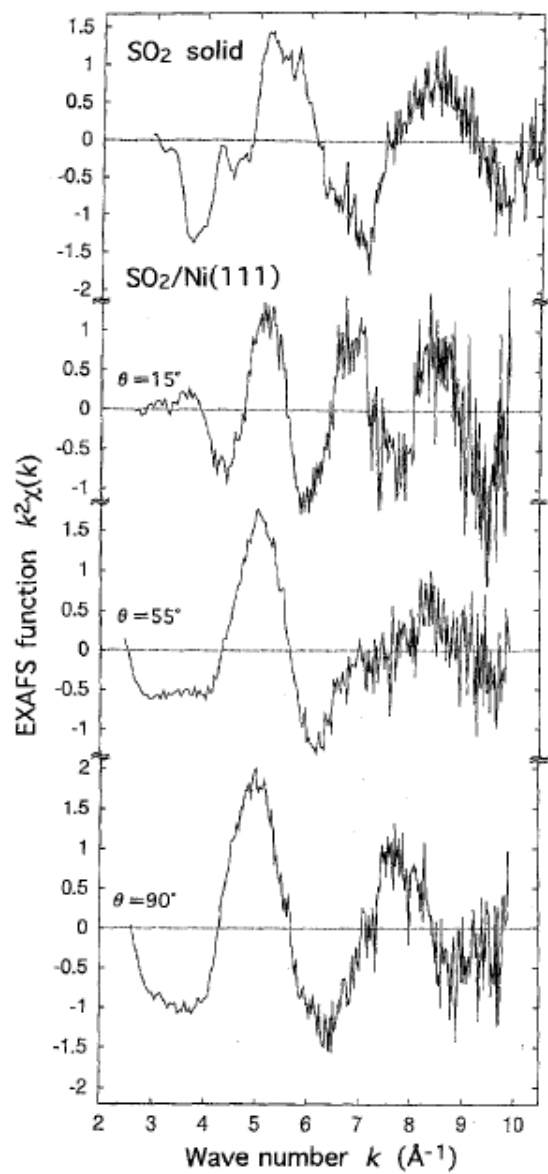


Fig. 4. S K-edge SEXAFS oscillation functions $k^2\chi(k)$ of submonolayer $\text{SO}_2/\text{Ni}(111)$ taken at X-ray incidence angles of $\theta \approx 90^\circ$, 55° and 15° at a temperature of 92 K, together with that of solid SO_2 at 92 K.

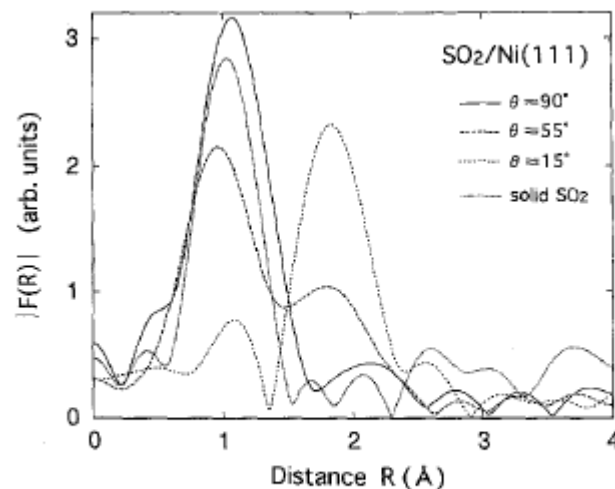


Fig. 6. Fourier transforms of $k^2\chi(k)$ of submonolayer $\text{SO}_2/\text{Ni}(111)$ and solid SO_2 shown in Fig. 4.

Note: S-O bond length : 1.43 Å (solid SO_2)

Using phase shift values from the references
and to determine the structure by fitting

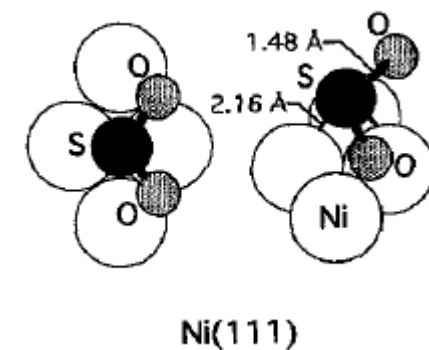
$$\chi(k) \propto \sum_j N_j \frac{1}{k r_j^2} \exp\{-2r_j/\lambda(k)\} \sin(2kr_j + \delta) \quad (\text{fitting})$$

Table 1

The ratio of the effective coordination numbers, $\eta = N^*(55^\circ)/N^*(15^\circ)$, for the S-Ni shells of $\text{SO}_2/\text{Ni}(111)$ and $\text{SO}_2/\text{Ni}(100)$, together with calculated values of η for typical adsorption sites on unreconstructed surfaces

| Surface | Experimental | Calculated | | |
|---------|--------------|------------|--------|-------|
| | | Hollow | Bridge | Atop |
| Ni(111) | 0.53(5) | 0.626 | 0.523 | 0.353 |
| Ni(100) | 0.51(5) | 0.966 | 0.522 | 0.353 |

For the calculations of η , S-Ni distances of 2.16 Å on Ni(111) and 2.18 Å on Ni(100) were used.



X-ray Magnetic Circular Dichroism (X線磁気円2色性)

$$\Delta\mu = \mu_+(+B) - \mu_+(-B) = \mu_-(-B) - \mu_-(+B) = \mu_-(-B) - \mu_+(-B) \quad (33)$$

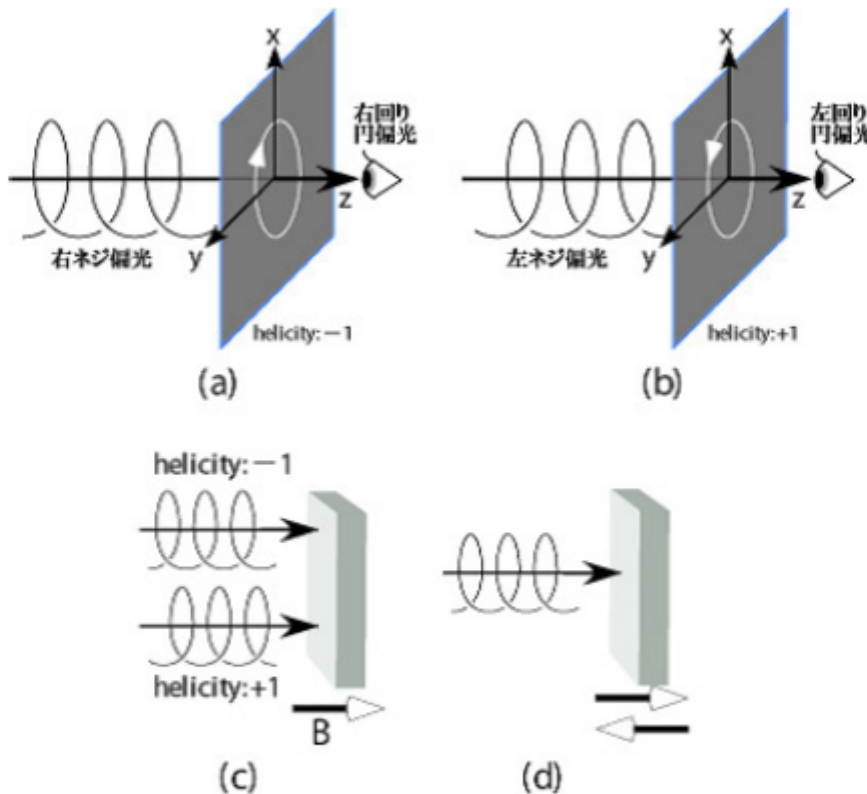


FIG. 21: (a,b) 円偏光の定義:(a) 右ネジ偏光、右回り円偏光、helicity=-1; (b) 左ネジ偏光、左回り円偏光、helicity=+1。 (c,d) XMCD の測定：(c) 円偏光の切換；(d) 印加磁場の向きの切換。

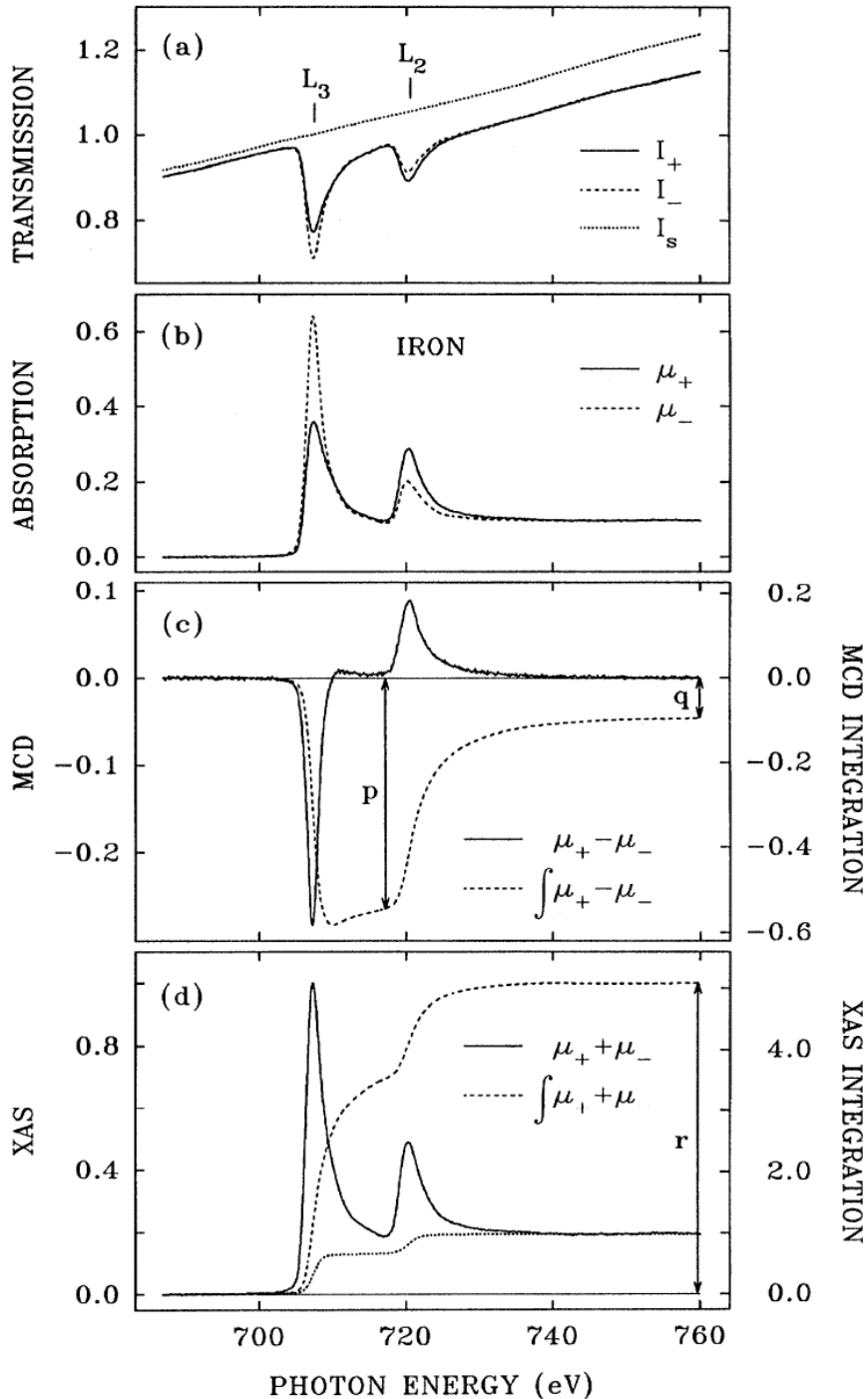


FIG. 1. $L_{2,3}$ -edge XAS and MCD spectra of iron: (a) transmission spectra of Fe/parylene thin films, and of the parylene substrates alone, taken at two opposite saturation magnetizations; (b) the XAS absorption spectra calculated from the transmission data shown in (a); (c) and (d) are the MCD and summed XAS spectra and their integrations calculated from the spectra shown in (b). The dotted line shown in (d) is the two-step-like function for edge-jump removal before the integration. The p and q shown in (c) and the r shown in (d) are the three integrals needed in the sum-rule analysis.

FIG. 24: Fe 試料における $L_{2,3}$ -吸収端 (edge) の XAS 及び XMCD スペクトル (積分)。(a) 実験で得られた透過スペクトル、(b)(a) から求めた XAS スペクトル、(c) XMCD スペクトルとその積分、(d) XAS スペクトルとその積分 [41]。 p, q, r を求めるための各積分は (d) の edge-jump を含むバックグラウンド (two-step-like function) を引いてから行われています。

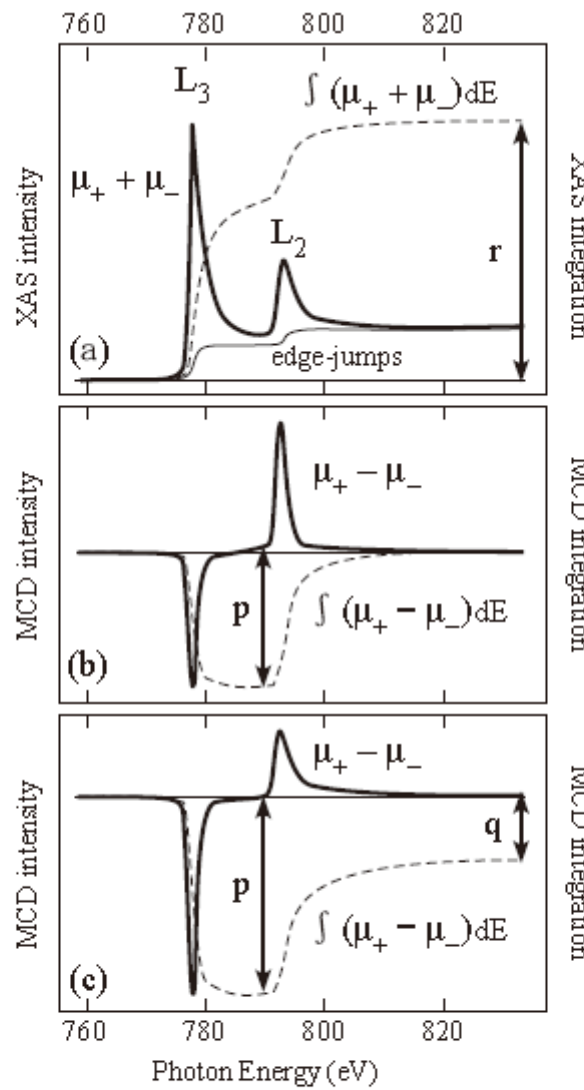
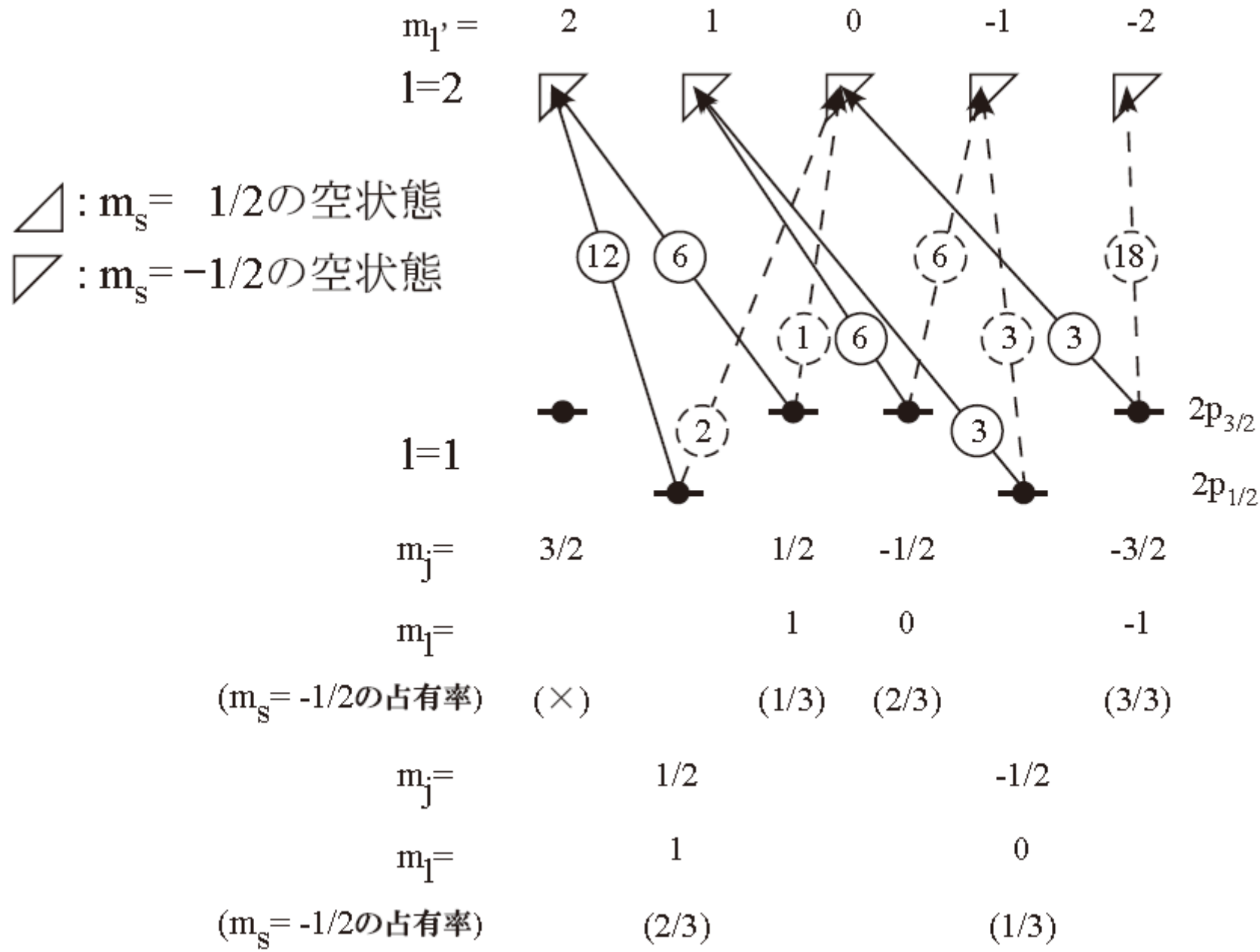
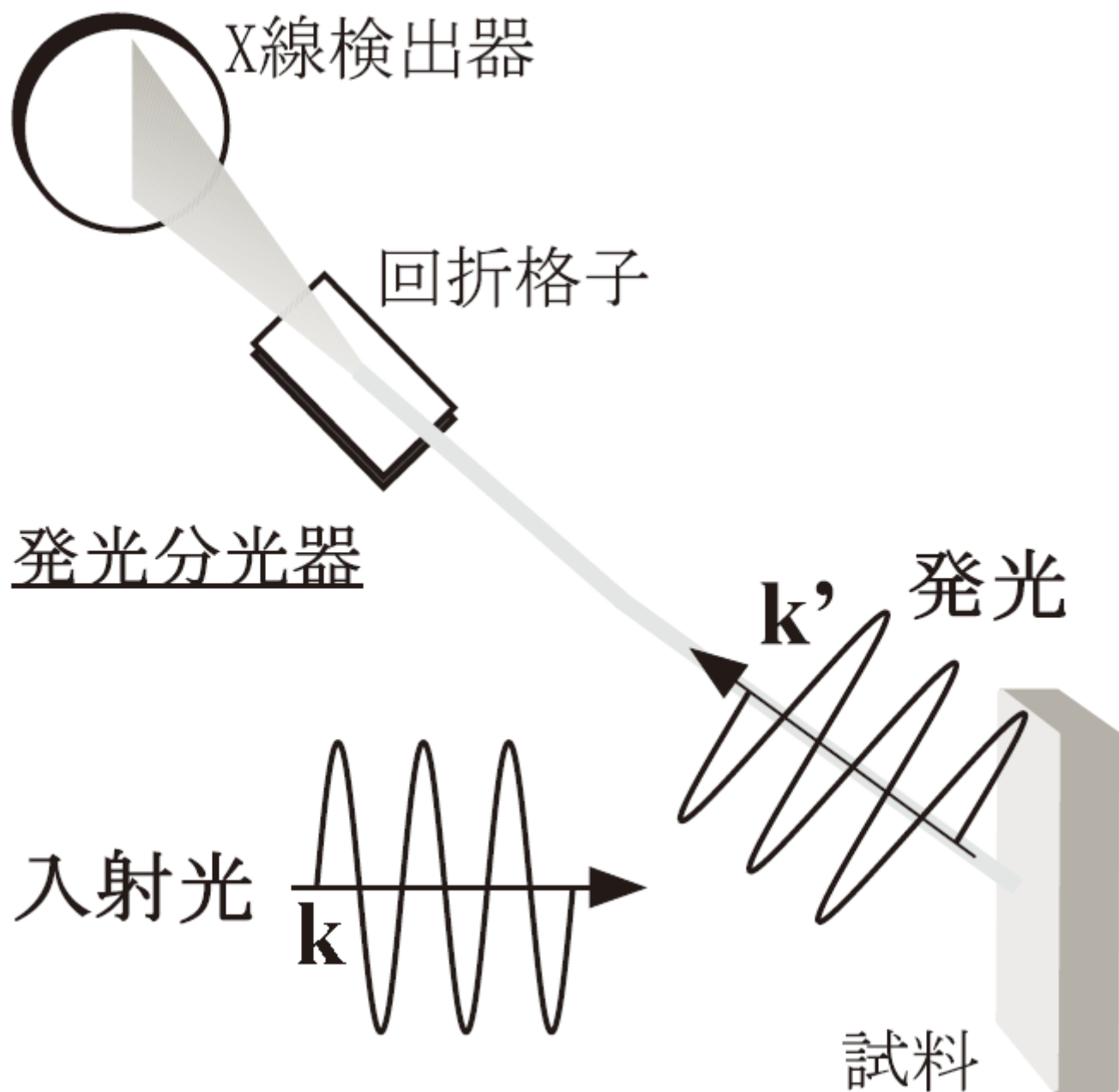
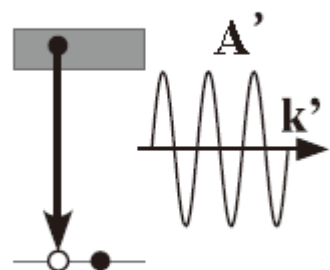


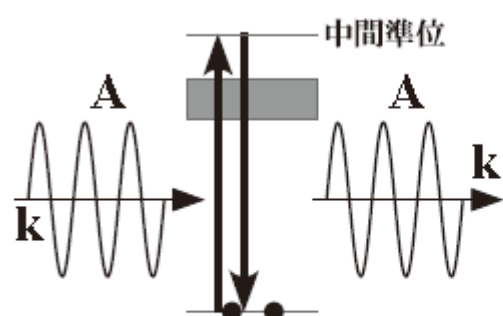
FIG. 23: $L_{2,3}$ -吸収端 (edge) の XAS 及び XMCD スペクトル (積分) と μ_+, μ_- の関係。 p, q, r を求めたための各種分は (a) の edge-jump を含むバックグラウンドを引いてから行われています。(a) $L_{2,3}$ -吸収端 (edge) の XAS スペクトルとその積分。(b) $L_{2,3}$ -吸収端 (edge) の XAS スペクトルとその積分 (軌道磁気モーメントが 0 の場合)。(c) $L_{2,3}$ -吸収端 (edge) の XAS スペクトルとその積分 (軌道磁気モーメントがある場合)。



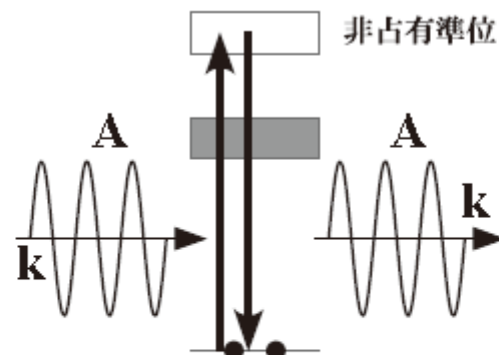




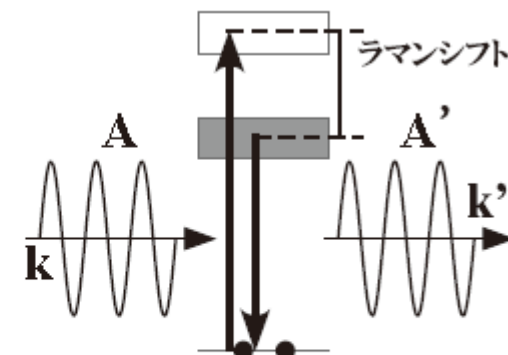
(c) 吸收:2次過程
(螢光過程)



(f) 弹性X線散乱
(レイリー散乱)



(g) 共鳴弾性X線散乱



(h) 共鳴非弾性X線散乱
(共鳴ラマン散乱)

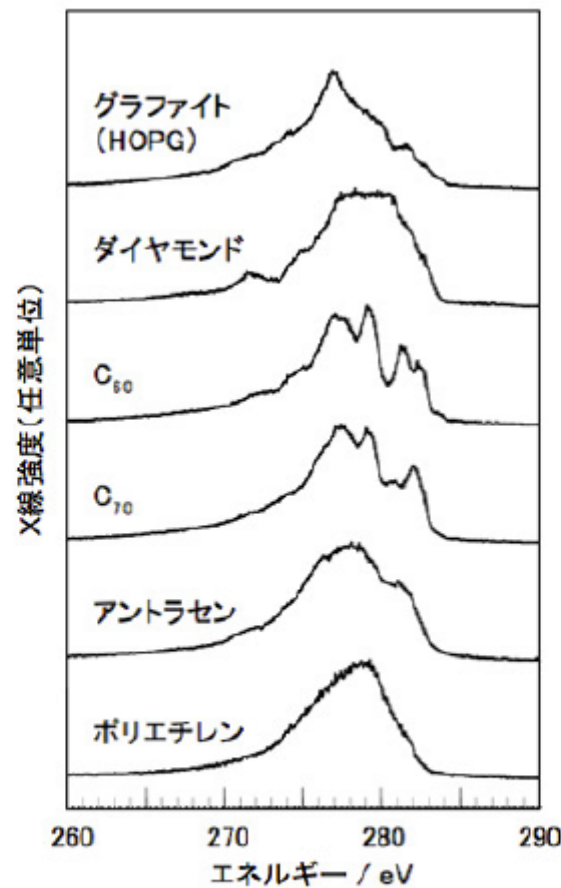


FIG. 26: 典型的な炭素化合物の放射光励起 CK X線発光(蛍光)スペクトル。(兵庫県立大: 村松康司教授より提供)

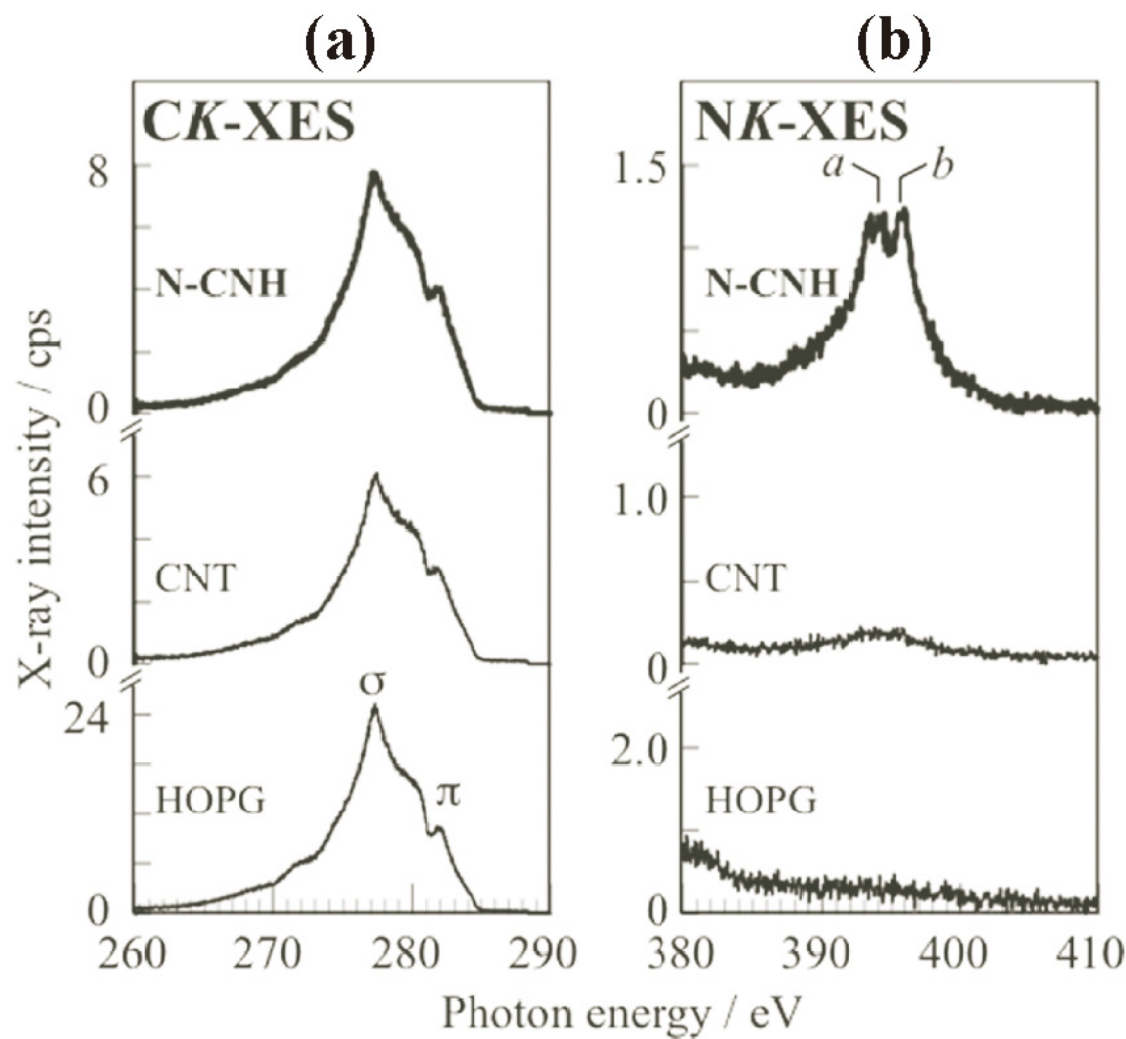


図 0.36 グラファイト (HOPG, Highly Oriented Pyrolytic Graphite)、カーボンナノチューブ (CNT, Carbon Nanotube)、窒素含有カーボンナノホーン (N-CNH, N-Carbon Nanohorn) の (a) 炭素及び (b) 窒素の K 裂の軟 X 線発光スペクトル³⁵⁾。励起光のエネルギーはそれぞれ 320 と 430 eV である。

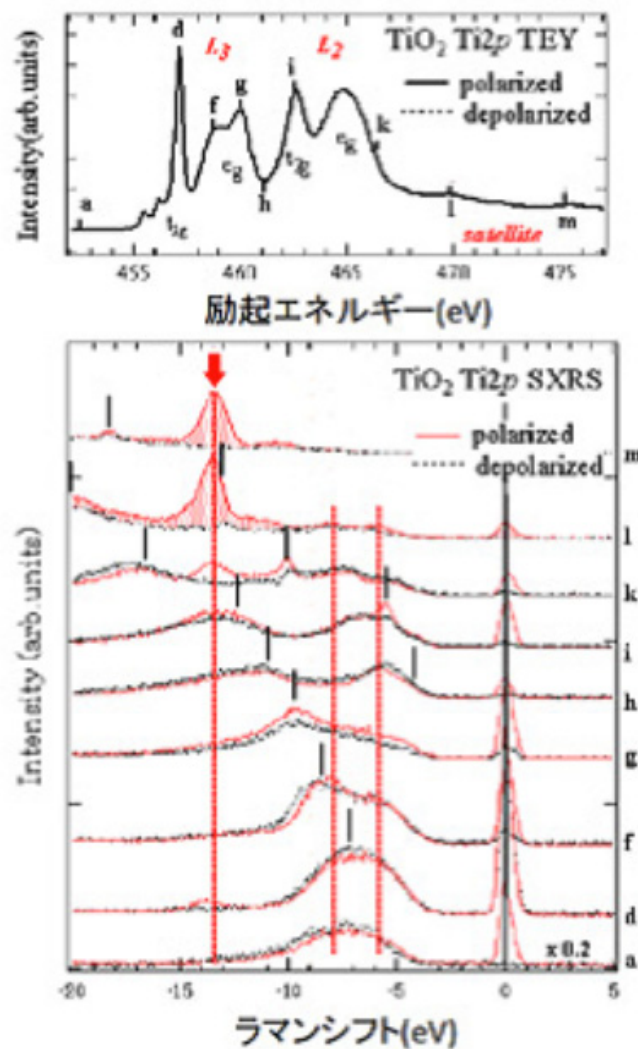
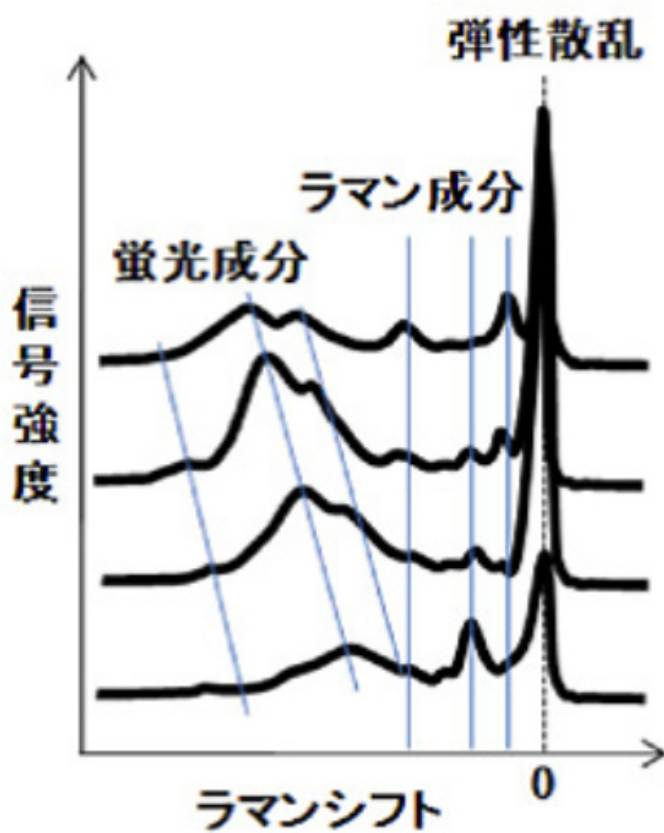
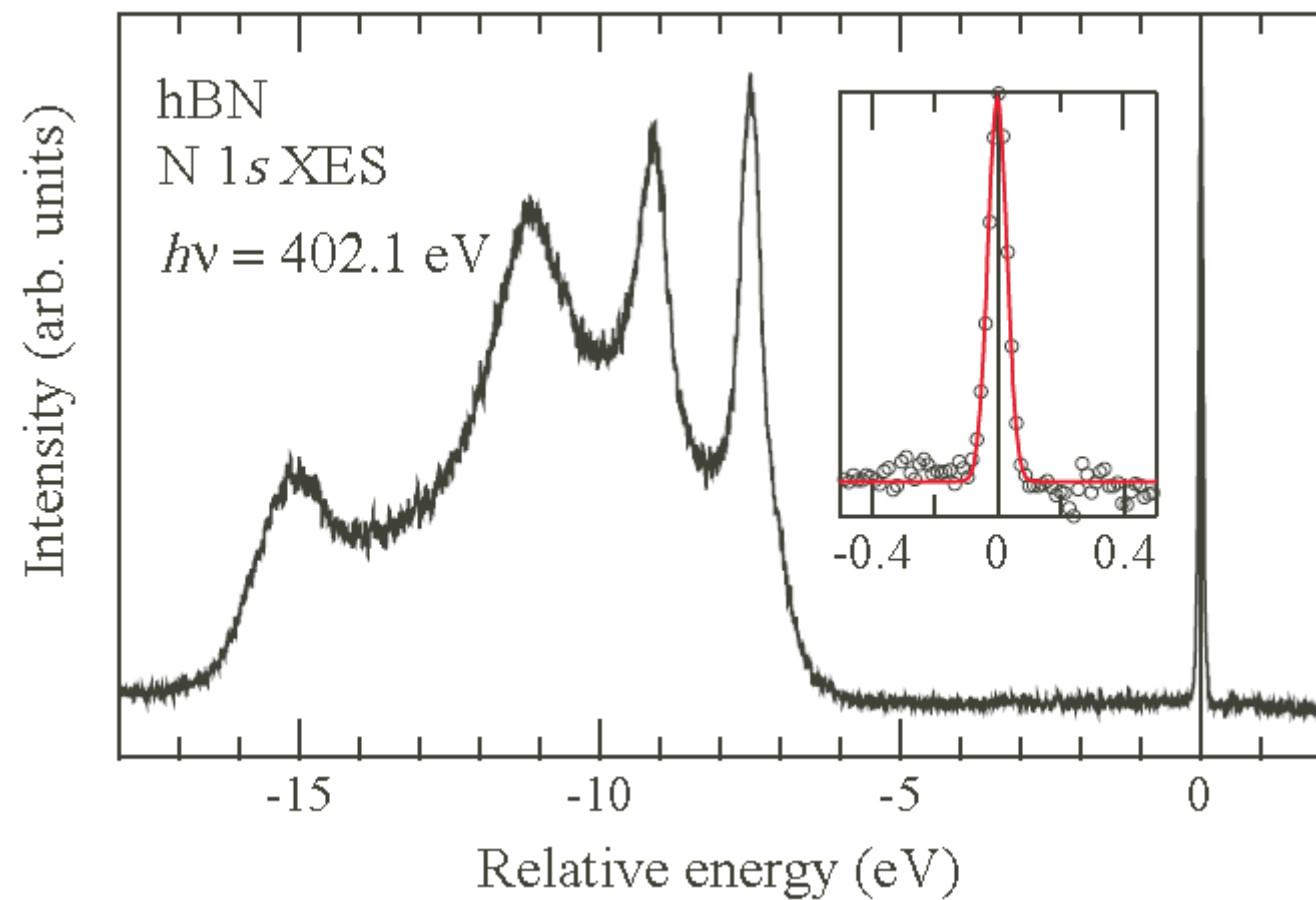


FIG. 27: (左) 共鳴励起発光の共鳴発光スペクトルのラマンシフト表示。(右) TiO_2 の $\text{Ti} 2p$ 共鳴発光スペクトル [47]。



Advantages of the resonant inelastic X-ray scattering(RIXS)

1. Exploiting both the energy and momentum dependence of the photon scattering cross section.
2. Element and orbital specific:
3. Bulk sensitive:
4. Needs only small sample volumes:
5. Utilize the polarization of the photon:

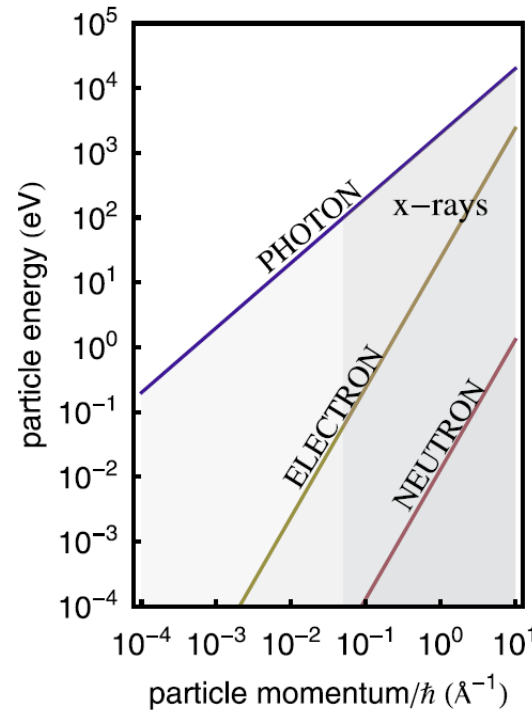
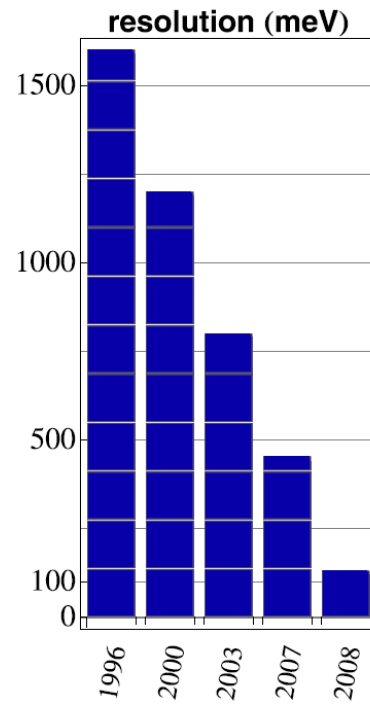
The main limitation is that the process is photon hungry;

■ 共鳴非弾性X線散乱・共鳴軟X線ラマン散乱

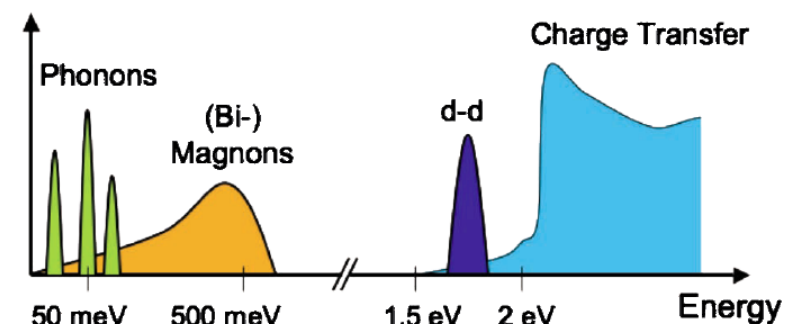
光源の高輝度化

エネルギーの高分解能化

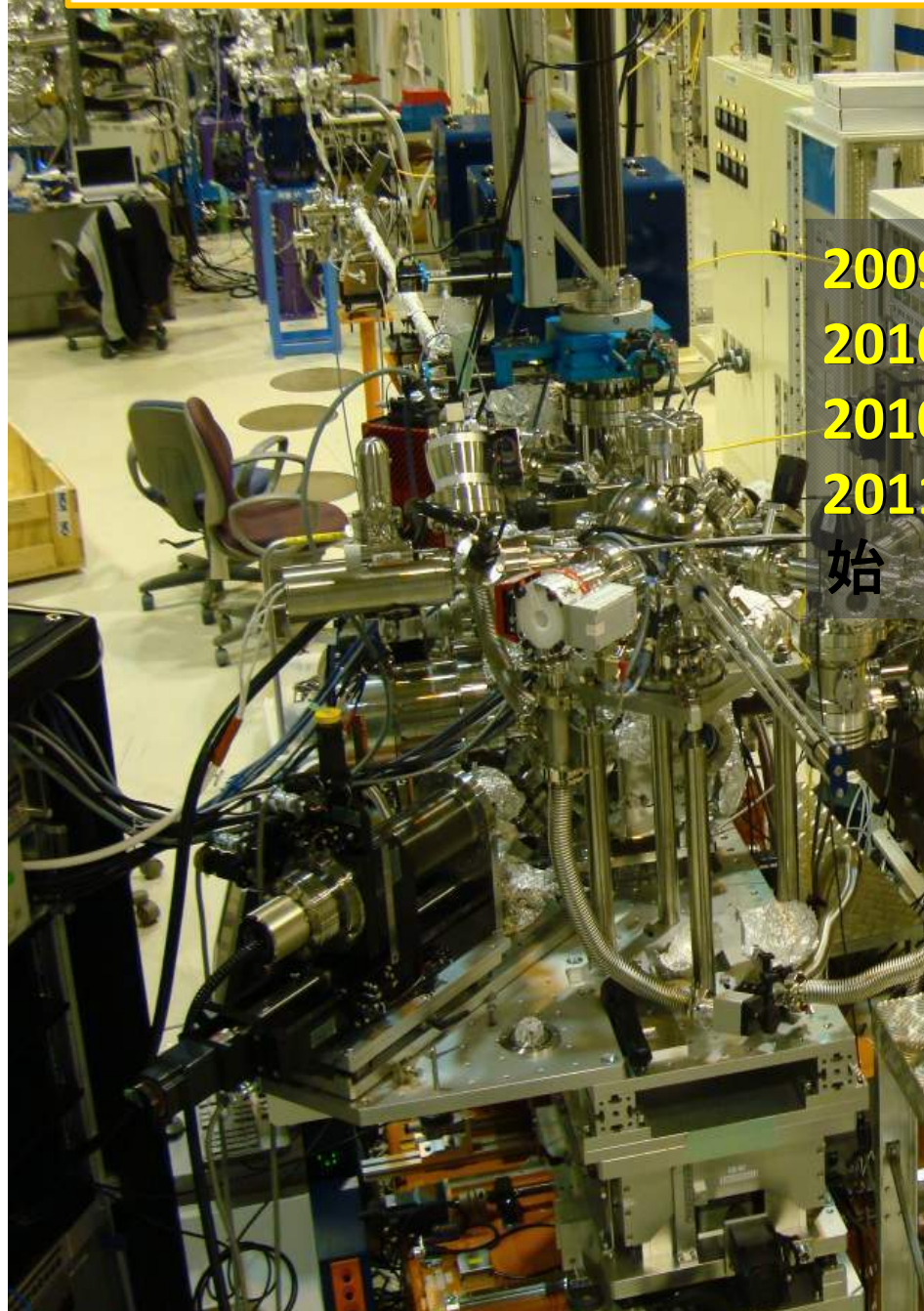
Soft x-ray regime: Cu L-edge



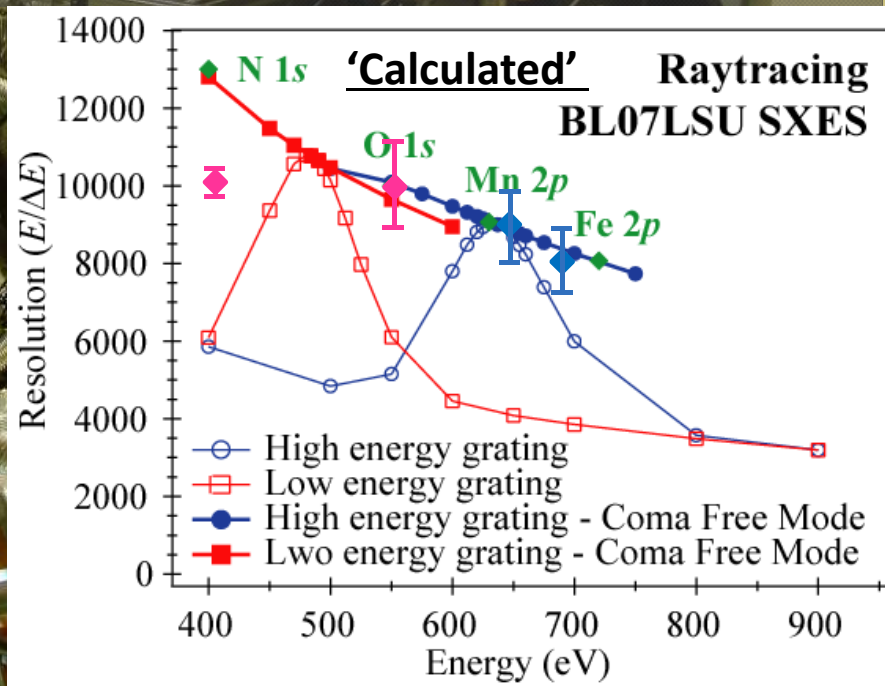
Different elementary excitations in condensed matter systems and their approximate energy scales in strongly correlated electron materials such as transition-metal oxides.



HORNET: Ultrahigh resolution XES station@SPring-8 BL07LSU



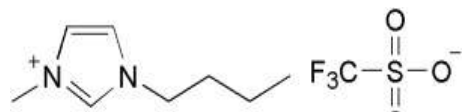
2009.10 コミッショニング
2010.7 分解能 $E/\Delta E > 5000$
2010.12 分解能 $E/\Delta E > 10000$ (N 1s)
2011.1~ ユーザー実験(G課題)開始
始



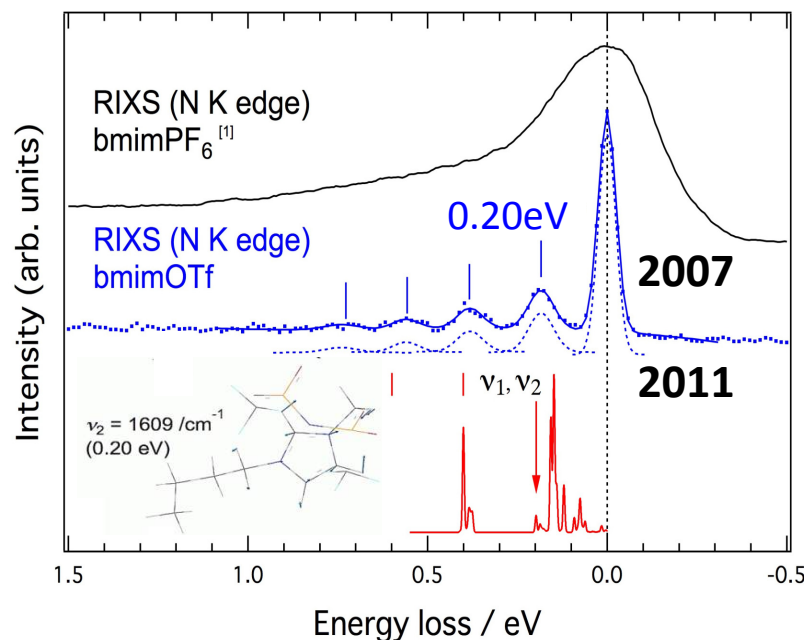
HORNET: Ultrahigh resolution XES station
@SPring-8 BL07LSU

UltraHigh-resolution

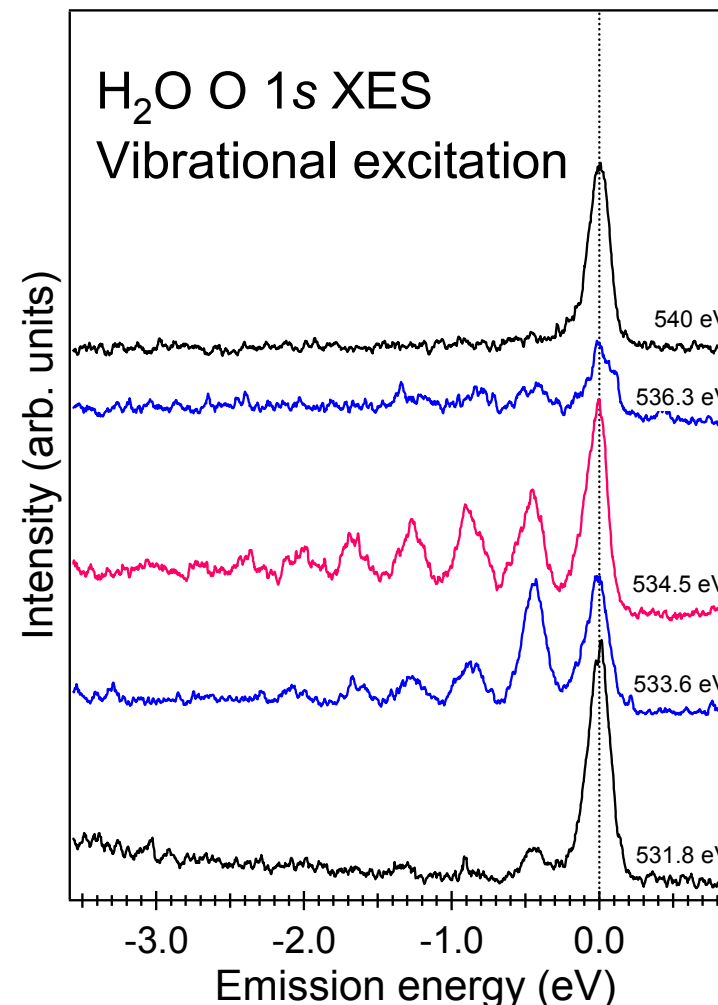
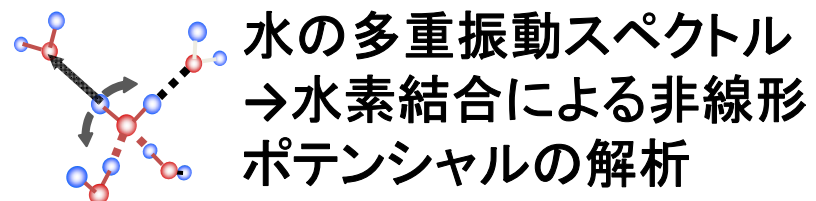
i) Ionic liquids



窒素周辺の多重振動スペクトル
→局所的な配位構造の情報



ii) liquid water



Synchrotron radiation facilities on the earth



XFEL facilities on the earth



SLAC

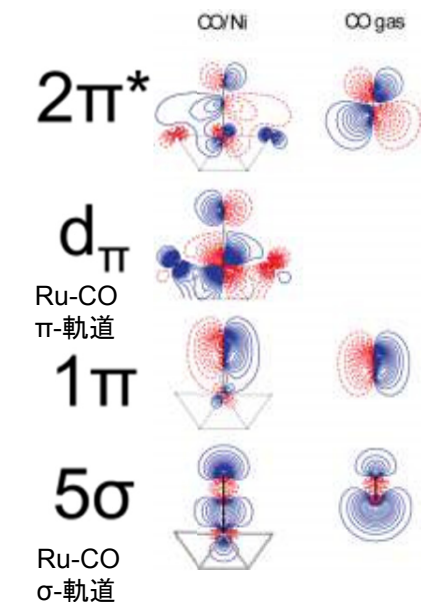
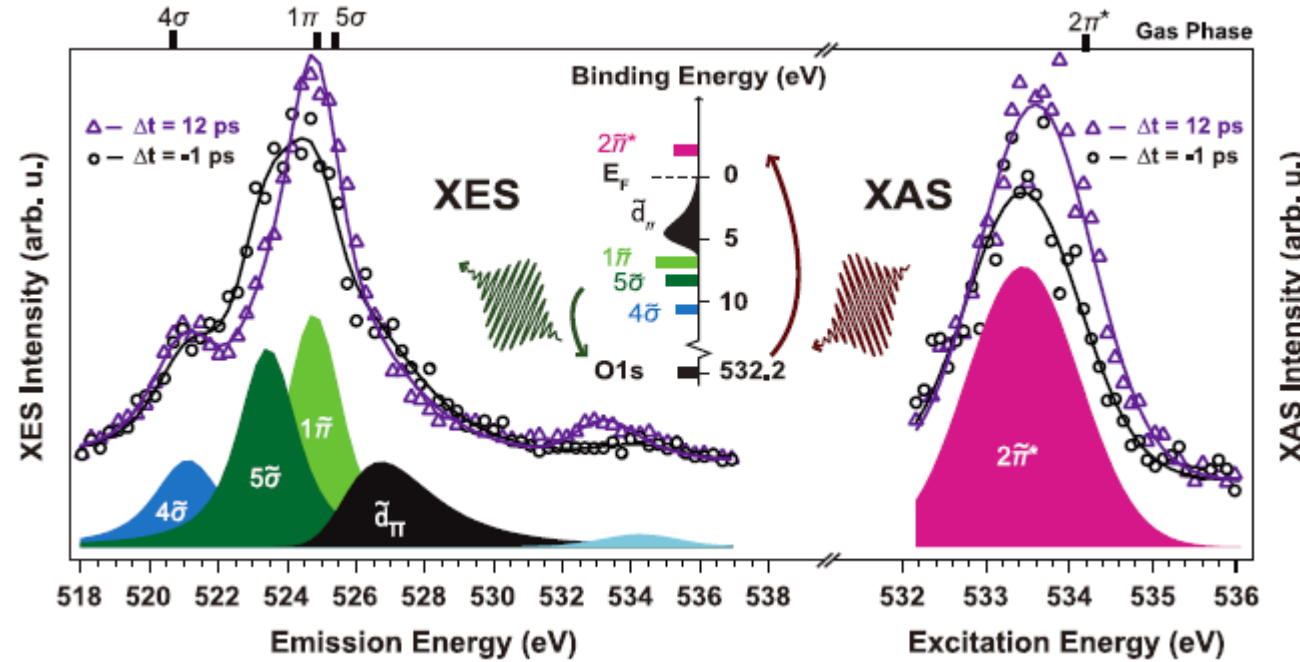
DESY

RIKEN/
SPring-8
SACLA

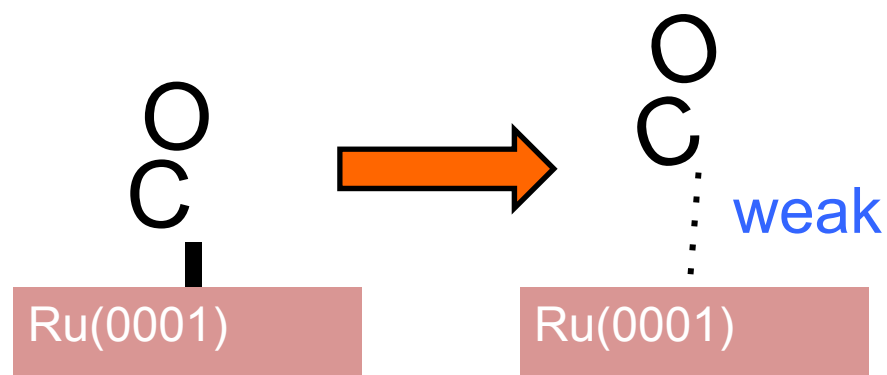
XES and XAS with XFEL CO desorption from Ru(0001) Pump-probe XES

LCLS@SLAC

M. Dell'Angela *et al.*, Science 339, 1302 (2013).



Direction observation
during chemical bond
breaking !

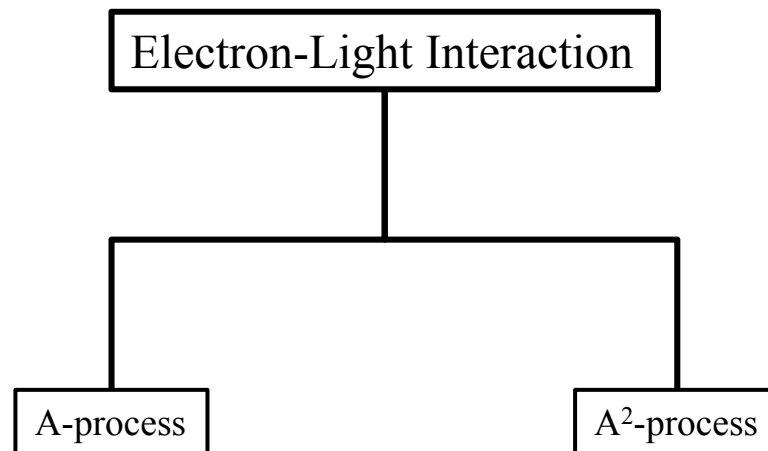


光物性物理学
Optical Properties and Spectroscopy of Solids

Light and Matter

Synchrotron radiation
Free Electron Laser

Solid (bulk and surface)



Electron-Light Interaction

Element and Chemical Species Analysis

Primary process

A-process

Secondary process

A^2 -process

Photoelectric effect

XPS
X-ray Photoelectron (Photoemission) Spectroscopy
CLS
Core-level Photoelectron (Photoemission) Spectroscopy

Fluorescence

Auger process (non-radiative)

Structure Determination

PED

Photoelectron Diffraction

XAFS

X-ray Absorption Fine Structure

Fluorescence Spectroscopy

AES

Auger Electron Spectroscopy

Electronic State Analysis

UPS

Ultraviolet Photoelectron (Photoemission) Spectroscopy

ARPES

Angle-resolved Photoelectron (Photoemission) Spectroscopy

EXAFS

Extended X-ray Absorption Fine Structure

AED

Auger Electron Diffraction

Spin and Magnetic Analysis

SARPES

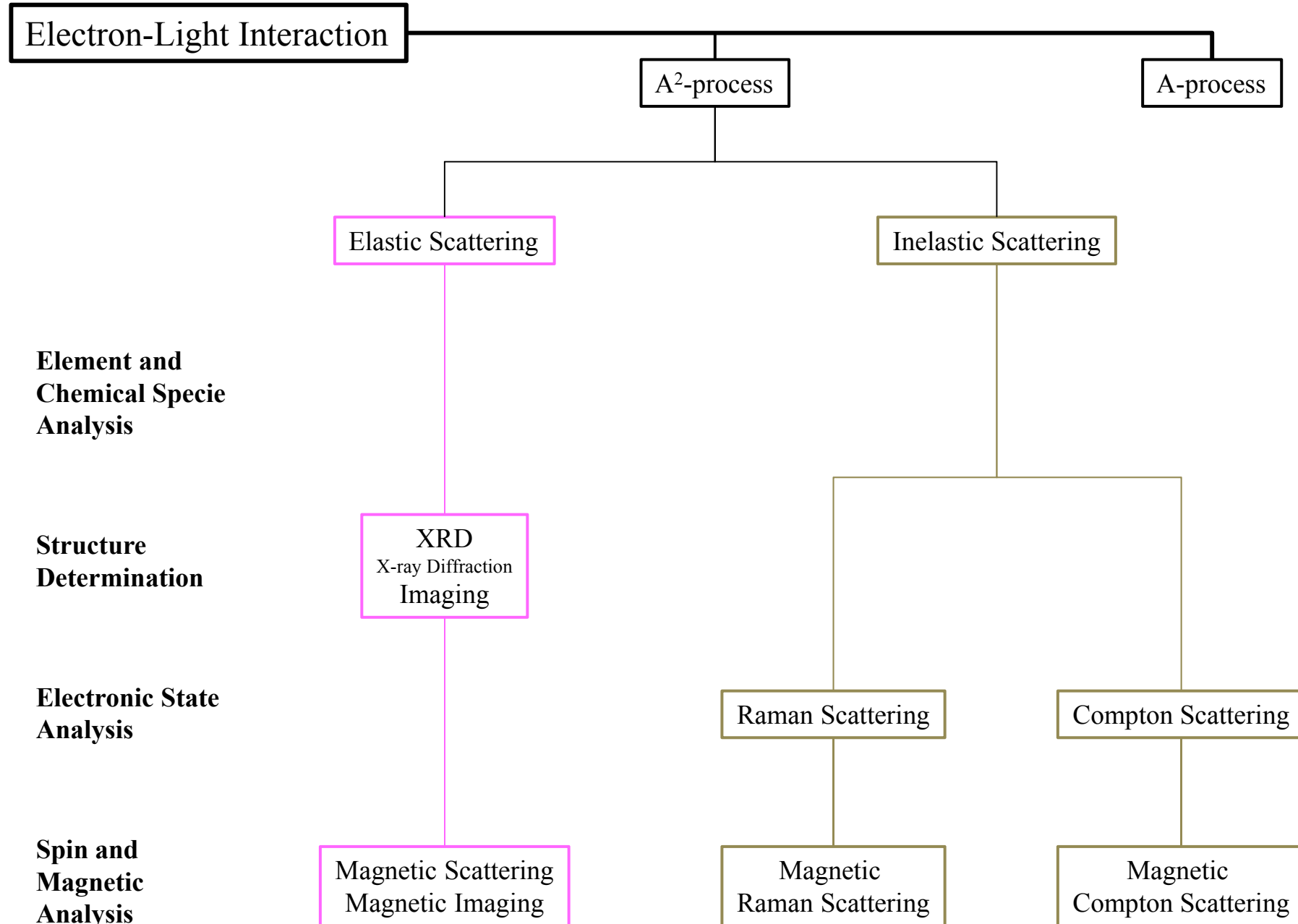
Spin- and Angle-Resolved Photoelectron (Photoemission) Spectroscopy

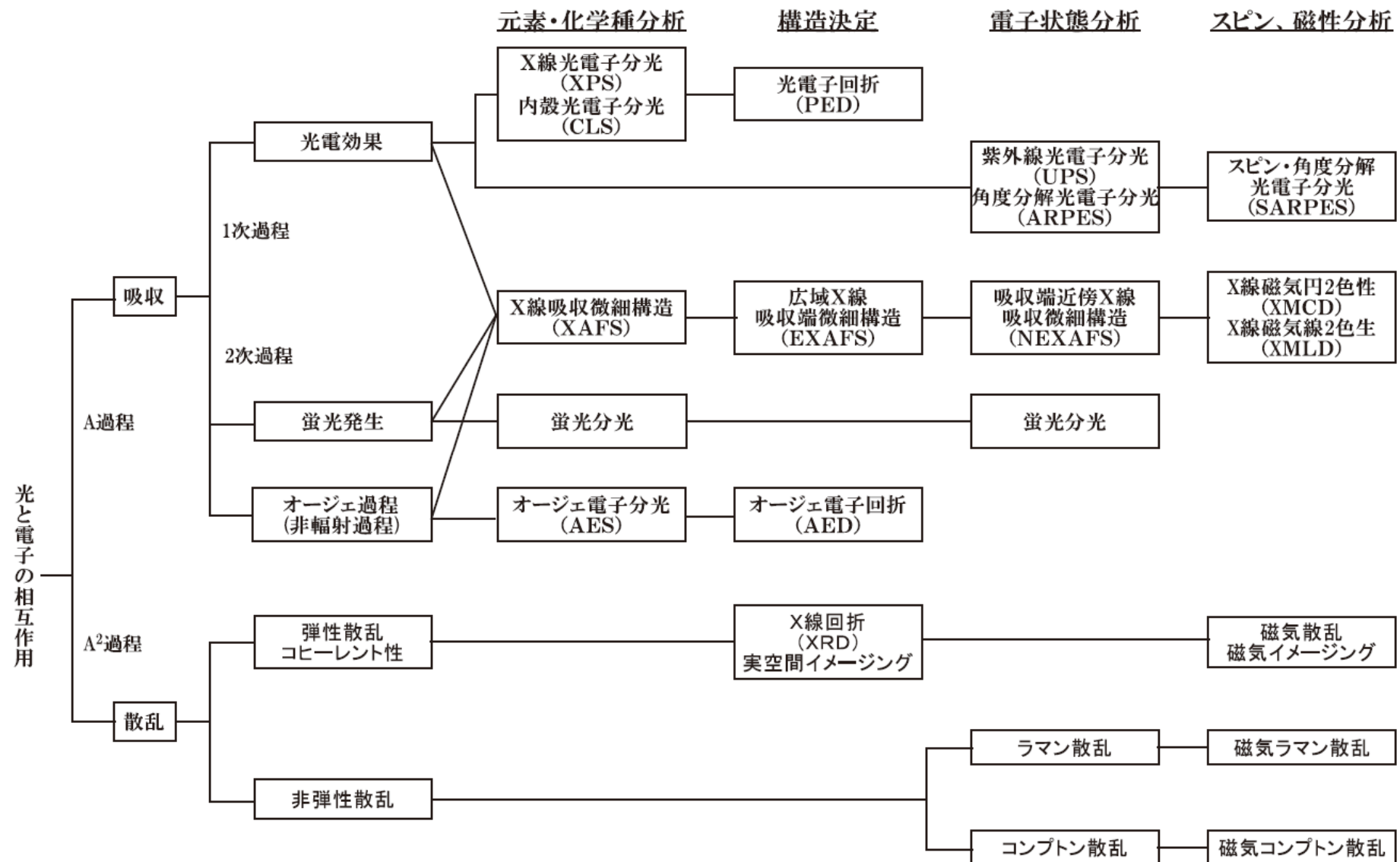
XMCD

X-ray Magnetic Circular Dichroism

XMLD

X-ray Magnetic Linear Dichroism





物質による軟X線の
吸収、散乱、発光を用いた
様々な分析法が存在し、
まとめるとこうなります。

みなさんが知りたい
物質情報は軟X線で
分かりそうですか？

